Urbanization drives genetic and plastic responses of the spotted jewelweed flower morphology

Jérôme Burkiewicz[1]*, Julie Carvalho[1], Sophie Caporgno[1], Joëlle Lafond[2,3]†, Céline Devaux[1,4], Étienne Normandin[1], Simon Joly[1,5]

[1]Institut de recherche en biologie végétale, Département de sciences biologiques, Université de Montréal; Montréal, H1X 2B2, Canada

[2]Département de sciences biologiques, Université de Montréal; Montréal, H2V 0B3, Canada

[3]Department of Zoology and Biodiversity Research Centre, University of British Columbia; Vancouver, V6T 1Z4, Canada

[4]Institut des Sciences de l'Évolution de Montpellier UMR 5554, Université de Montpellier; Montpellier, 34095, France

[5]Jardin Botanique de Montréal; Montréal, H1X 2B2, Canada

* Corresponding author. Email: jerome.burkiewicz@umontreal.ca

Abstract

The spectacular diversity of flowers is strongly driven by pollinator-mediated selection that favors attractive flowers and effective pollen transfer. We tested how urbanization affected the genetic and plastic components of flower morphology of *Impatiens capensis* across four Canadian cities, accounting for changes in abiotic conditions and pollinator communities. Urbanization altered the species composition of pollinator communities and bumblebee size – the main pollinator, but the size effect varied among cities. Urbanization also impacted flower size through both genetic and plastic responses. In particular, the genetic component of the sepal size – a tubular floral organ in which pollinators enter to access the nectar – correlated positively with bumblebee size. These results suggest that urbanization, by changing pollinator communities, drives evolutionary changes in flower morphology.

Main text

Flowers show an astounding diversity in shapes, sizes, colors, and scents across angiosperms, mostly resulting from selection imposed by pollinators (*1–6*). Flowers can genetically adapt to changes in pollinator communities or abundance by evolving traits that enhance attraction, such as color, scent and nectar, that facilitate pollen transfer by improving the mechanical fit with pollinators through shape or size modifications, or promote self-pollination (*7–9*). But flowers can also be modified by their environment through phenotypic plasticity (*10*, *11*), which can be either

adaptive or maladaptive depending on whether the environment modifies the phenotype in a way that increases or decreases the mean fitness of the population, respectively (*12*). Also, phenotypic plasticity can hide genetic adaptation if it affects the phenotype in a way that opposes natural selection, a concept called counter-gradient variation (*13*, *14*). Despite the important roles of genetics and phenotypic plasticity in determining phenotypes, few studies have tried to tease them apart when investigating evolutionary responses of flower morphology across environmental gradients.

Urban environments offer a unique opportunity to study evolutionary responses to environmental changes (*15*). The development and spread of cities alter abiotic conditions by remodeling the physical environment and biotic conditions through their effects on species richness, abundance, interactions, and evolution (*15–18*). Furthermore, since urban habitats are generally more similar to each other than to their surrounding natural environments (*17*), studying species response to urbanization in different cities is equivalent to a replicated evolutionary experiment (*19*), and could uncover parallel or idiosyncratic responses across cities (*17*, *20*). Urbanization is expected to disrupt mutualistic interactions, such as pollination, because these interactions require synchrony between flowering and pollinator activity and phenotype matching between the plant and pollinator traits (*21*, *22*). Pollinator communities and phenotypes commonly exhibit changes along urban gradients (*23–28*), and such changes, as well as those in the abiotic environments, can drive flower evolution through both genetic and plastic responses. Yet, few studies have investigated the impact of urbanization on the evolution of flower traits while also considering changes in pollinator communities (*29–31*), and none have attempted to disentangle genetic from plastic responses.

We tested whether urbanization impacts, directly or indirectly through its effects on pollinator communities, the size and shape of flowers of the spotted jewelweed, *Impatiens capensis* Meerb. This annual species has a mixed pollination strategy, bearing both closed, green, and tiny self-fertilizing (cleistogamous) flowers, and, open, orange, large protandrous and mainly outcrossing (chasmogamous) flowers (Fig. 1D). This reproductive strategy is plastic, as a greater proportion of chasmogamous flowers are produced with more light (*32*, *33*), but it does not seem to be affected by urbanization (*34*). Populations of *I. capensis* growing in sunlight produce numerous chasmogamous flowers pollinated by bumblebees, bees, wasps, flies, and hummingbirds (*35–37*), which all feed on pollen or the nectar secreted in the spur. The spur curvature of *I. capensis* is heritable, and affects pollen removal by hummingbirds (*38*) and the duration of visits by bees (*39*). *I. capensis* evolved smaller sepals under relaxed selection (*40*), and larger flowers under pollinator limitation (*41*). Also, flower shape and size were correlated with urbanization intensity in Montreal, Canada (*42*). Finally, reproductive success was shown to be limited by pollen deposition in urban and

natural habitats (*34*), potentially allowing natural selection to drive floral phenotypic changes (*43*). Therefore, the generalist pollination strategy of *I. capensis*, and its reported capacity to respond to its pollinator communities in both urban and natural habitats make it an excellent system for studying the evolution of flower shape and size in response to urbanization.

To test whether urbanization impacts the pollinator communities of *Impatiens capensis* and its flower shape and size, we performed both field investigations and a greenhouse common garden experiment to control for environmental effects. We considered the phenotypes measured in the common garden as the genetic components of the corresponding traits, whereas the phenotypes measured in the field corresponded to joint genetic and plastic components of the traits. We quantified flower shapes and sizes, and we characterized pollinator communities for a total of 16 populations, paired by habitat – urban versus natural – in and around four large Canadian cities ("regions" hereafter): Toronto, Ottawa, Montreal and Quebec (Fig. 1A). Field surveys were conducted in 2021 and 2022, while the common garden experiment was performed in 2022 using seeds collected in the field in 2021. We studied populations of *I. capensis* growing in sunlight to focus on the evolutionary responses of their animal-pollinated flowers. We analyzed 1870 flowers (Table S1), 692 net-captured pollinators, and 124 hours of video-recorded pollination observations to quantify the impact of urbanization on the genetic and plastic components of flower morphology, and the composition of pollinator communities.

Urban and natural populations, across the four regions studied, were characterized by different abiotic environments, showing our ability to discriminate those environments in the field and justifying the use of the "habitat" categorical variable in all analyses that quantify the effects of urbanization (Fig. 1 and Fig. S1). The natural populations were associated with higher tree cover and greater vegetation index (NDVI; Normalized Difference Vegetation Index), whereas urban populations were associated with higher proportions of impervious surfaces and built areas, as well as lower isothermality (day-to-night temperature variation compared to annual oscillations) due to a heat island effect (Fig. 1B, C and Fig. S1).

Urbanization modifies the pollinator communities of *I. capensis*

To assess whether variation in local pollinator communities could select for different flower morphologies, we collected the pollinators of *I. capensis* from 15 populations in 2021 and 16 populations in 2022. On two different days, we spent 20 minutes net-catching specimens that had made contact with the anthers or the stigma of the flowers. We

also recorded pollinator visits on camera for 2 hours the same two days. We estimated pollinator visitation rates as the number of pollination events per flower per hour.

Bumblebees (*Bombus* spp.) were the most frequent pollinators of *I. capensis*, representing 73% of all pollination events recorded on video (Fig. 2A). *Bombus impatiens* was the most collected specimen (62.4%, Table S2), followed by *Bombus vagans* (12.7%, Table S2). *Apis mellifera* represented 6.4% of the specimens sampled (Table S2) but primarily collected pollen and may not be a reliable pollinator, as stigmas are not receptive when anthers are mature. *Anthophora terminalis*, *Vespidae*, and *Augochlora pura* together represented 12.5% of the specimens collected (Table S2), and these less common and less cosmopolitan pollinators did not make contact as consistently with the reproductive structures as bumblebees, according to video recordings.

Pollinator communities of *I. capensis* differed between urban and natural habitats ($R^2_{adj} = 0.264$, $P = 0.013$; Fig. 2B, Fig. S2). Urban habitats were more associated with *Bombus impatiens, Vespula maculifrons,* and *Apis mellifera,* while natural habitats were more associated with *Bombus vagans*, *Augochlora pura* and *Rhingia nasica* (Fig. 2B, Fig. S2). Among these pollinators, bumblebees were the most consistently found across all populations, and as such, they best characterized urban and natural pollinator communities of *I. capensis.* Finally, we found that the effect of urbanization on pollinator visitation rates varied among regions (Region × Habitat: $F_{(3, 23)} = 3.675$, $P = 0.026$; Table S3A, B).

Urban environments could affect the body size of insect pollinators via changes in the pollinator species composition or through evolutionary responses to changes in resource availability and temperature (*44*). So far, studies have produced conflicting results regarding how urbanization affects bumblebee sizes (*27*, *28*). A greater distance between resource patches, as commonly found in cities, could favor larger insects with greater flight capacities (*45*). On the other hand, high temperatures could favor smaller insects with greater thermoregulation potential (*28*). In either case, pollinator size differences have the potential to affect selection on flower morphology. Using the inter-tegular distance (ITD) as a proxy of bumblebee size and flight capacity (*45*, *46*), we found that the effect of urbanization on bumblebee size varied among regions (Region × Habitat: $\chi^2_{(3)} = 8.826$, $P = 0.031$; Fig. 2C, D, Table S5A), with Quebec showing the strongest effect (11.6% increase from natural to urban populations, Fig. 2C, D, Table S5B).

Urbanization affects the flower size of *I. capensis* through plastic and genetic effects

In *I. capensis*, pollinators must pass through the tubular, orange, large posterior sepal to access the nectar produced in the spur (Fig. 3A). We thus assumed that the size of the sepal could ensure the effective contact between pollinators and the reproductive parts of the flower that are located at the top entrance of the sepal. As bumblebee size varied among populations, we tested whether this trait could select for sepal size to maintain an optimal mechanical fit with their pollinators and maximize pollen transfer. We first compared the sepal size of *I. capensis* between habitats in our common garden experiment and in the field to decipher the genetic and plastic components of the trait. We then tested whether the genetic component of the sepal size was positively correlated with bumblebee size.

Sepal size was the same for urban and natural populations in the field ($\chi^2_{(1)} = 0.239$, P = 0.624; Fig. S3, Table S6C). However, in the common garden experiment, sepals from urban populations were on average 7.6% larger than those in natural populations ($\chi^2_{(1)} = 8.564$, P = 0.003; Table S7A), though this effect varied among regions (Region × Habitat: $\chi^2_{(3)} = 8.329$, P = 0.039; Table S7A), with Quebec populations showing the largest difference (20.3% increase, $t_{(7.29)} = 3.700$, P = 0.028; Fig. 3B, C, Table S7B). Together, these results suggest that phenotypic plasticity in the field could hide the genetic differences in sepal size between habitats. To further investigate this phenotypic plasticity, we analyzed the mean response of sepal size per habitat to changes in the environment (field vs. common garden). Compared to the common garden experiment, the sepal size measured in the field was smaller in urban populations and larger in natural populations, thus completely masking the existing genetic differences in sepal size between habitats (Environment × Habitat, 2021: $\chi^2_{(1)} = 4.796$, P = 0.028; 2022: $\chi^2_{(1)} = 3.706$, P = 0.054; Fig. 3D, Fig. S4A, Table S8). Finally, we found that the genetic component of the mean sepal size per population was positively correlated with the mean population bumblebee size ($F_{(1,11)} = 6.531$, P = 0.026, $R^2_{adj} = 0.527$; Fig. 4, Table S9). These results suggest that bumblebee size is a general selection agent for sepal size. Hence, the direction of the plastic response measured opposes natural selection in urban environments, especially in populations characterized by larger bumblebees (e.g. Quebec, Montreal) (Fig. 3B, C, Fig. S6).

The corolla surface of *I. capensis* likely represents an attraction function and not a mechanical fit function. Previous studies indicated that increased competition for flower resources (*47*) and reduced pollen dispersal in urban environments (*30*) should result in stronger pollen limitation (*48*). Therefore, selection should favor larger floral displays in pollinator-limited populations to better attract pollinators (*49*, *50*). We thus hypothesized that pollinator visitation rates would negatively correlate with the genetic component of the corolla surface, which is one component of the floral display.

In the field, corolla surface was affected by habitat, but only in certain regions and certain years, suggesting phenotypic plasticity (Table S6C). Under controlled conditions, the effect of urbanization on corolla surface varied among regions (Region × Habitat: $\chi^2_{(3)} = 8.136$, P = 0.043; Fig. 3F, G, Table S7A). The corolla surface was 19% larger in the field compared to the common garden, regardless of habitat, confirming strong phenotypic plasticity for this trait (2021: $\chi^2_{(1)} = 8.859$, P = 0.002; 2022: $\chi^2_{(1)} = 36.761$, P < 0.001; Fig. 3H, Fig. S4B, Table S8). This plasticity could be caused by developmental constraints, weather conditions, and pollinator visits (by pushing the petals apart), and may at least partly explain the variation among years (Table S6C), and between field and controlled conditions. The genetic component of the corolla surface was positively correlated with pollinator visitation rates in urban populations, but not in natural populations (Pollinator Visitation Rate × Habitat: $F_{(1,11)} = 14.851$, P = 0.002; Fig. S7, Table S10).

Urbanization affects the flower shape of *I. capensis* through plastic responses

Because urbanization impacted *I. capensis* pollinator communities and bumblebee size, we further assessed if these factors affected flower shape as another strategy to promote efficient pollen removal and deposition in each habitat. We used geometric morphometrics to explain variation in flower shape (with flower size removed), and permutational multivariate analysis of variance (PERMANOVA or Procrustes ANOVA) to compare the corolla and sepal shapes between urban and natural habitats, both under controlled conditions and in the wild, accounting for allometry, year, sex stage of the flower, and region.

The spur of urban flowers was shorter and less curved compared to the ones in natural habitats in the field ($F_{(1,1518)} = 3.751$, P = 0.019; Fig. 5B, C, Table S11A), but not in controlled conditions ($F_{(1,315)} = 0.858$, P = 0.502; Fig. 5B, C, Table S11A). In contrast, corolla shape was similar in urban and natural habitats, both in the common garden ($F_{(1,314)} = 0.436$, P = 0.837; Fig. 5E, Table S11A) and in the field ($F_{(1,1509)} = 0.886$, P = 0.472; Fig. 5F, Table S11A). These contrasting results suggest that urbanization impacted the sepal shape only through phenotypic plasticity, although the statistical power to detect genetic response was small for the common garden experiment (Table S1). Corolla shape of flowers from the field populations also differed from those raised in the common garden (Environment: $F_{(1,1839)} = 6.198$, P = 0.002; Fig. 5E, F, Table S11B), further supporting the effect of phenotypic plasticity on flowers. The shape of flowers in controlled conditions suggests that they are less open than those in the field (Fig. 5E).

Genetic and plastic responses, and a possible common mechanism for sepal size

The combination of fieldwork and common garden experiments across four cities in southeastern Canada revealed that urbanization altered the pollinator community of *I. capensis* and its flower morphology. We found that urbanization affected the flower size and shape through both plastic and genetic responses. Nectar spurs were shorter and less curved spurs in urban habitats than in natural habitats, a consequence of phenotypic plasticity. The genetic component of sepal size was overall larger in urban areas, despite variation among cities, whereas the effect of urbanization on corolla surface showed different trends in different cities. More importantly, we found that the genetic component of sepal size was positively correlated with bumblebee size across populations, in both urban and natural habitats. This suggests that despite substantial phenotypic plasticity in the field that sometimes masked the genetic determination of sepal size, as well as the existence of discrepancies among regions, we potentially found a common mechanism that explains variation in sepal size of *I. capensis* across urbanization gradients where sepal size has to fit the size of its bumblebee pollinators to maximize pollen transfer.

Corolla surface was positively correlated with pollinator visitation rates in urban populations, contrary to our expectation that larger corollas should be favored in environments with reduced pollination services. However, this finding does not preclude the expected negative relationship between floral display and pollen limitation. Our analysis was limited to a single component of floral display—corolla surface, excluding the effect of flower number, and one aspect of pollen limitation, as we did not assess pollen transfer effectiveness and pollen quality. Trade-offs may also play a role; for example, limited resources could constrain investment in both flower size and number, such that increased flower number compensates for smaller corollas in overall display. Pollinator visitation rates to *I. capensis* may also be driven by the entire plant community through both competitive and facilitated interactions with co-flowering species. For instance, the presence of the large-flowered invasive *Impatiens glandulifera* has been associated with selection for reduced corolla height in *I. capensis* (*51*).

For both sepal size and corolla surface, the impact of urbanization was not the same across cities, but they aligned with the impact of urbanization on pollinator communities. For example, pollinators were the largest in urban populations of Quebec, where the genetic component of flower size was the most impacted by urbanization. Previous studies on flower evolution in urban areas have focused on phenotypic changes associated with pollinator availability and pollen movement (*29*, *31*), but they left aside a more thorough characterization of pollinator communities. Here, we show that characterizing the pollinator community helps to understand the floral evolution in an urbanization context.

Phenotypic plasticity can be adaptive or maladaptive depending on whether it moves phenotypes towards or away from the fitness optimum of populations. It can also decrease the efficiency of natural selection as the phenotypes with the highest fitness represent both the genetic and plastic components of the corresponding traits. We found that for sepal size of *I. capensis*, phenotypic plasticity masked the genetic differences detected in the common garden experiment (Fig. 3D; Fig S4), suggesting a counter-gradient variation in which plasticity typically modifies the phenotype in a direction opposite to natural selection (*13*). Assuming a similar plastic response for all genotypes, such as larger flowers in the common garden are also larger in the field conditions, we infer that the sepal size genetically respond to its pollinator community. Therefore, bumblebee selection for sepal size along an urbanization gradient appears to be a case of compensatory adaptive change in which selection counteracts the homogenizing effect of phenotypic plasticity (*13*, *14*, *52*). Indeed, natural selection seems to favor larger flowers in some cities because of the presence of larger bumblebees, but plasticity masked the genetic differences in the field (Fig. 3D, Fig. S4). We also highlighted that the corolla size and shape were also significantly affected by the environment through phenotypic plasticity, which is particularly evident from the observed differences between the common garden and field conditions. Very few urban evolution studies quantified phenotypic plasticity (but see (*53*)), and our results demonstrate that it is critical to investigate it to fully understand the causes of phenotypic changes and adequately interpret the evolutionary responses of plants to environmental changes (*54*).

Strong environmental changes associated with urbanization impact living organisms, their interactions, and their evolution. Although our knowledge of eco-evolutionary dynamics in these environments has increased in the last decade, integrative approaches that assess plastic and genetic components of traits while considering species interactions are still scarce, but they are necessary to understand rapid evolution to changing environments. Only with this will we be able to understand adaptation to urbanization and pave the way for conservation policies in these habitats.

References and Notes

1. G. L. Stebbins, Adaptive Radiation of Reproductive Characteristics in Angiosperms, I: Pollination Mechanisms. *Annual Review of Ecology and Systematics* **1**, 307–326 (1970).

2. C. Galen, Why do flowers vary?: The functional ecology of variation in flower size and form within natural plant populations. *BioScience* **49**, 631–640 (1999).

3. J. B. Whittall, S. A. Hodges, Pollinator shifts drive increasingly long nectar spurs in columbine flowers. *Nature* **447**, 706–709 (2007).

4. T. van der Niet, S. D. Johnson, Phylogenetic evidence for pollinator-driven diversification of angiosperms. *Trends in Ecology & Evolution* **27**, 353–361 (2012).

5. J. Ollerton, R. Winfree, S. Tarrant, How many flowering plants are pollinated by animals? *Oikos* **120**, 321–326 (2011).

6. L. D. Harder, S. D. Johnson, Darwin's beautiful contrivances: evolutionary and functional evidence for floral adaptation. *New Phytologist* **183**, 530–545 (2009).

7. J. M. Gómez, M. Abdelaziz, J. P. M. Camacho, A. J. Muñoz-Pajares, F. Perfectti, Local adaptation and maladaptation to pollinators in a generalist geographic mosaic. *Ecology Letters* **12**, 672–682 (2009).

8. D. D. L. Gervasi, F. P. Schiestl, Real-time divergent evolution in plants driven by pollinators. *Nature Communications* **8**, 14691 (2017).

9. S. Acoca-Pidolle, P. Gauthier, L. Devresse, A. Deverge Merdrignac, V. Pons, P.-O. Cheptou, Ongoing convergent evolution of a selfing syndrome threatens plant–pollinator interactions. *New Phytologist* **242**, 717–726 (2024).

10. C. M. Caruso, Plasticity of inflorescence traits in Lobelia siphilitica (Lobeliaceae) in response to soil water availability. *American Journal of Botany* **93**, 531–538 (2006).

11. J. M. Gómez, F. Perfectti, C. Armas, E. Narbona, A. González-Megías, L. Navarro, L. DeSoto, R. Torices, Within-individual phenotypic plasticity in flowers fosters pollination niche shift. *Nature Communications* **11**, 4019 (2020).

12. T. Dorey, F. P. Schiestl, Plant phenotypic plasticity changes pollinator-mediated selection. *Evolution* **76**, 2930–2944 (2022).

13. D. O. Conover, E. T. Schultz, Phenotypic similarity and the evolutionary significance of countergradient variation. *Trends in Ecology & Evolution* **10**, 248–252 (1995).

14. D. O. Conover, T. A. Duffy, L. A. Hice, The covariance between genetic and environmental influences across ecological gradients. *Annals of the New York Academy of Sciences* **1168**, 100–129 (2009).

15. M. T. J. Johnson, J. Munshi-South, Evolution of life in urban environments. *Science* **358**, eaam8327 (2017).

16. M. L. McKinney, Effects of urbanization on species richness: A review of plants and animals. *Urban Ecosystems* **11**, 161–176 (2008).

17. J. S. Santangelo, R. W. Ness, B. Cohan, C. R. Fitzpatrick, S. G. Innes, S. Koch, L. S. Miles, S. Munim, P. R. Peres-Neto, C. Prashad, A. T. Tong, W. E. Aguirre, P. O. Akinwole, M. Alberti, J. Álvarez, J. T. Anderson, J. J. Anderson, Y. Ando, N. R. Andrew, F. Angeoletto, D. N. Anstett, J. Anstett, F. Aoki-Gonçalves, A. Z. A. Arietta, M. T. K. Arroyo, E. J. Austen, F. Baena-Díaz, C. A. Barker, H. A. Baylis, J. M. Beliz, A. Benitez-Mora, D. Bickford, G. Biedebach, G. S. Blackburn, M. M. A. Boehm, S. P. Bonser, D. Bonte, J. R. Bragger, C. Branquinho, K. I. Brans, J. C. Bresciano, P. D. Brom, A. Bucharova, B. Burt, J. F. Cahill, K. D. Campbell, E. J. Carlen, D. Carmona, M. C. Castellanos, G. Centenaro, I. Chalen, J. A. Chaves, M. Chávez-Pesqueira, X.-Y. Chen, A. M. Chilton, K. M. Chomiak, D. F. Cisneros-Heredia, I. K. Cisse, A. T. Classen, M. S. Comerford, C. C. Fradinger, H. Corney, A. J. Crawford, K. M. Crawford, M. Dahirel, S. David, R. De Haan, N. J. Deacon, C. Dean, E. del-Val, E. K. Deligiannis, D. Denney, M. A. Dettlaff, M. F. DiLeo, Y.-Y. Ding, M. E. Domínguez-López, D. M. Dominoni, S. L. Draud, K. Dyson, J. Ellers, C. I. Espinosa, L. Essi, M. Falahati-Anbaran, J. C. F. Falcão, H. T. Fargo, M. D. E. Fellowes, R. M. Fitzpatrick, L. E. Flaherty, P. J. Flood, M. F. Flores, J. Fornoni, A. G. Foster, C. J. Frost, T. L. Fuentes, J. R. Fulkerson, E. Gagnon, F. Garbsch, C. J.

Garroway, A. C. Gerstein, M. M. Giasson, E. B. Girdler, S. Gkelis, W. Godsoe, A. M. Golemiec, M. Golemiec, C. González-Lagos, A. J. Gorton, K. M. Gotanda, G. Granath, S. Greiner, J. S. Griffiths, F. Grilo, P. E. Gundel, B. Hamilton, J. M. Hardin, T. He, S. B. Heard, A. F. Henriques, M. Hernández-Poveda, M. C. Hetherington-Rauth, S. J. Hill, D. F. Hochuli, K. A. Hodgins, G. R. Hood, G. R. Hopkins, K. A. Hovanes, A. R. Howard, S. C. Hubbard, C. N. Ibarra-Cerdeña, C. Iñiguez-Armijos, P. Jara-Arancio, B. J. M. Jarrett, M. Jeannot, V. Jiménez-Lobato, M. Johnson, O. Johnson, P. P. Johnson, R. Johnson, M. P. Josephson, M. C. Jung, M. G. Just, A. Kahilainen, O. S. Kailing, E. Kariñho-Betancourt, R. Karousou, L. A. Kirn, A. Kirschbaum, A.-L. Laine, J. M. LaMontagne, C. Lampei, C. Lara, E. L. Larson, A. Lázaro-Lobo, J. H. Le, D. S. Leandro, C. Lee, Y. Lei, C. A. León, M. E. Lequerica Tamara, D. C. Levesque, W.-J. Liao, M. Ljubotina, H. Locke, M. T. Lockett, T. C. Longo, J. T. Lundholm, T. MacGillavry, C. R. Mackin, A. R. Mahmoud, I. A. Manju, J. Mariën, D. N. Martínez, M. Martínez-Bartolomé, E. K. Meineke, W. Mendoza-Arroyo, T. J. S. Merritt, L. E. L. Merritt, G. Migiani, E. S. Minor, N. Mitchell, M. Mohammadi Bazargani, A. T. Moles, J. D. Monk, C. M. Moore, P. A. Morales-Morales, B. T. Moyers, M. Muñoz-Rojas, J. Munshi-South, S. M. Murphy, M. M. Murúa, M. Neila, O. Nikolaidis, I. Njunjić, P. Nosko, J. Núñez-Farfán, T. Ohgushi, K. M. Olsen, Ø. H. Opedal, C. Ornelas, A. L. Parachnowitsch, A. S. Paratore, A. M. Parody-Merino, J. Paule, O. S. Paulo, J. C. Pena, V. W. Pfeiffer, P. Pinho, A. Piot, I. M. Porth, N. Poulos, A. Puentes, J. Qu, E. Quintero-Vallejo, S. M. Raciti, J. A. M. Raeymaekers, K. M. Raveala, D. J. Rennison, M. C. Ribeiro, J. L. Richardson, G. Rivas-Torres, B. J. Rivera, A. B. Roddy, E. Rodriguez-Muñoz, J. R. Román, L. S. Rossi, J. K. Rowntree, T. J. Ryan, S. Salinas, N. J. Sanders, L. Y. Santiago-Rosario, A. M. Savage, J. F. Scheepens, M. Schilthuizen, A. C. Schneider, T. Scholier, J. L. Scott, S. A. Shaheed, R. P. Shefferson, C. A. Shepard, J. A. Shykoff, G. Silveira, A. D. Smith, L. Solis-Gabriel, A. Soro, K. V. Spellman, K. S. Whitney, I. Starke-Ottich, J. G. Stephan, J. D. Stephens, J. Szulc, M. Szulkin, A. J. M. Tack, Í. Tamburrino, T. D. Tate, E. Tergemina, P. Theodorou, K. A. Thompson, C. G. Threlfall, R. M. Tinghitella, L. Toledo-Chelala, X. Tong, L. Uroy, S. Utsumi, M. L. Vandegehuchte, A. VanWallendael, P. M. Vidal, S. M. Wadgymar, A.-Y. Wang, N. Wang, M. L. Warbrick, K. D. Whitney, M. Wiesmeier, J. T. Wiles, J. Wu, Z. A. Xirocostas, Z. Yan, J. Yao, J. B. Yoder, O. Yoshida, J. Zhang, Z. Zhao, C. D. Ziter, M. P. Zuellig, R. A. Zufall, J. E. Zurita, S. E. Zytynska, M. T. J. Johnson, Global urban environmental change drives adaptation in white clover. *Science* **375**, 1275–1281 (2022).

18. M. Alberti, C. Correa, J. M. Marzluff, A. P. Hendry, E. P. Palkovacs, K. M. Gotanda, V. M. Hunt, T. M. Apgar, Y. Zhou, Global urban signatures of phenotypic change in animal and plant populations. *Proceedings of the National Academy of Sciences* **114**, 8951 (2017).

19. J. S. Santangelo, L. S. Miles, S. T. Breitbart, D. Murray-Stoker, L. R. Rivkin, M. T. J. Johnson, R. W. Ness, "Urban Environments as a Framework to Study Parallel Evolution" in *Urban Evolutionary Biology* (Oxford University Press, Oxford, 2020), pp. 36–53.

20. S. E. Diamond, L. D. Chick, A. Perez, S. A. Strickler, R. A. Martin, Evolution of thermal tolerance and its fitness consequences: parallel and non-parallel responses to urban heat islands across three cities. *Proceedings of the Royal Society B: Biological Sciences* **285**, 20180036 (2018).

21. R. E. Irwin, E. Youngsteadt, P. S. Warren, J. L. Bronstein, "The Evolutionary Ecology of Mutualisms in Urban Landscapes" in *Urban Evolutionary Biology* (Oxford University Press, Oxford, 2020), pp. 111–129.

22. A. Fisogni, N. Hautekèete, Y. Piquot, M. Brun, C. Vanappelghem, D. Michez, F. Massol, Urbanization drives an early spring for plants but not for pollinators. *Oikos* **129**, 1681–1691 (2020).

23. K. C. R. Baldock, M. A. Goddard, D. M. Hicks, W. E. Kunin, N. Mitschunas, H. Morse, L. M. Osgathorpe, S. G. Potts, K. M. Robertson, A. V. Scott, P. P. A. Staniczenko, G. N. Stone, I. P. Vaughan, J. Memmott, A systems approach reveals urban pollinator hotspots and conservation opportunities. *Nature Ecology & Evolution* **3**, 363–373 (2019).

24. D. M. Hall, G. R. Camilo, R. K. Tonietto, J. Ollerton, K. Ahrné, M. Arduser, J. S. Ascher, K. C. R. Baldock, R. Fowler, G. Frankie, D. Goulson, B. Gunnarsson, M. E. Hanley, J. I. Jackson, G. Langellotto, D. Lowenstein, E. S. Minor, S. M. Philpott, S. G. Potts, M. H. Sirohi, E. M. Spevak, G. N. Stone, C. G. Threlfall, The city as a refuge for insect pollinators. *Conservation Biology* **31**, 24–29 (2017).

25. A. Wenzel, I. Grass, V. V. Belavadi, T. Tscharntke, How urbanization is driving pollinator diversity and pollination – A systematic review. *Biological Conservation* **241**, 108321 (2020).

26. P. Theodorou, R. Radzevičiūtė, G. Lentendu, B. Kahnt, M. Husemann, C. Bleidorn, J. Settele, O. Schweiger, I. Grosse, T. Wubet, T. E. Murray, R. J. Paxton, Urban areas as hotspots for bees and pollination but not a panacea for all insects. *Nature Communications* **11**, 576 (2020).

27. P. Theodorou, L. M. Baltz, R. J. Paxton, A. Soro, Urbanization is associated with shifts in bumblebee body size, with cascading effects on pollination. *Evolutionary Applications* **14**, 53–68 (2021).

28. H. Eggenberger, D. Frey, L. Pellissier, J. Ghazoul, S. Fontana, M. Moretti, Urban bumblebees are smaller and more phenotypically diverse than their rural counterparts. *Journal of Animal Ecology* **88**, 1522–1533 (2019).

29. R. E. Irwin, P. S. Warren, L. S. Adler, Phenotypic selection on floral traits in an urban landscape. *Proceedings of the Royal Society B: Biological Sciences* **285**, 20181239 (2018).

30. L. R. Rivkin, V. J. Nhan, A. E. Weis, M. T. J. Johnson, Variation in pollinator-mediated plant reproduction across an urbanization gradient. *Oecologia* **192**, 1073–1083 (2020).

31. A. Ushimaru, A. Kobayashi, I. Dohzono, Does urbanization promote floral diversification? implications from changes in herkogamy with pollinator availability in an urban-rural area. *The American Naturalist* **184**, 258–267 (2014).

32. D. M. Waller, Environmental determinants of outcrossing in Impatiens capensis (Balsaminaceae). *Evolution* **34**, 747–761 (1980).

33. D. W. Schemske, Evolution of reproductive characteristics in Impatiens (Balsaminaceae): the significance of cleistogamy and chasmogamy. *Ecology* **59**, 596–613 (1978).

34. C. A. Barker, R. D. Sargent, Pollination Services to Impatiens Capensis (Balsaminaceae) Are Maintained across an Urbanization Gradient. *International Journal of Plant Sciences*, 000–000 (2020).

35. C. B. Fenster, W. S. Armbruster, P. Wilson, M. R. Dudash, J. D. Thomson, Pollination Syndromes and Floral Specialization. *Annual Review of Ecology, Evolution, and Systematics* **35**, 375–403 (2004).

36. R. W. Rust, Pollination in Impatiens capensis and Impatiens pallida (Balsaminaceae). *Bulletin of the Torrey Botanical Club* **104**, 361–367 (1977).

37. R. W. Rust, Pollination of Impatiens capensis: pollinators and nectar robbers. *Journal of the Kansas Entomological Society* **52**, 297–308 (1979).

38. S. E. Travers, E. J. Temeles, I. Pan, The relationship between nectar spur curvature in jewelweed (Impatiens capensis) and pollen removal by hummingbird pollinators. *Canadian Journal of Botany* **81**, 164–170 (2003).

39. H. J. Young, Selection on spur shape in Impatiens capensis. *Oecologia* **156**, 535–543 (2008).

40. Y. Zhao, D. J. Schoen, Relaxed selection and the evolution of the chasmogamous flower of Impatiens capensis (Balsaminaceae). *Evolutionary Ecology* **36**, 233–250 (2022).

41. H. Panique, C. M. Caruso, Simulated pollinator declines intensify selection on floral traits that facilitate selfing and outcrossing in Impatiens capensis. *American Journal of Botany* **107**, 148–154 (2020).

42. J. Faure, V. Volz, S. Joly, Variation in flower size and shape of Impatiens capensis is correlated with urbanization in Montreal, Canada. *Ecology and Evolution* **13**, e10826 (2023).

43. L. D. Harder, M. A. Aizen, Floral adaptation and diversification under pollen limitation. *Philosophical Transactions of the Royal Society B: Biological Sciences* **365**, 529–543 (2010).

44. D. Goulson, *Bumblebees: Behaviour, Ecology, and Conservation* (Oxford University Press, 2010).

45. S. S. Greenleaf, N. M. Williams, R. Winfree, C. Kremen, Bee foraging ranges and their relationship to body size. *Oecologia* **153**, 589–596 (2007).

46. J. H. Cane, Estimation of bee size using intertegular span (Apoidea). *Journal of the Kansas Entomological Society* **60**, 145–147 (1987).

47. E. I. Hennig, J. Ghazoul, Plant–pollinator interactions within the urban environment. *Perspectives in Plant Ecology, Evolution and Systematics* **13**, 137–150 (2011).

48. A. Zink, P. J. CaraDonna, K. Larsen, A. M. Iler, Pollination deficits increase with urbanization in Chicago. *Ecosphere* **15**, e70100 (2024).

49. B. Geslin, B. Gauzens, E. Thébault, I. Dajoz, Plant Pollinator Networks along a Gradient of Urbanisation. *PLOS ONE* **8**, e63421 (2013).

50. M. Thomann, E. Imbert, C. Devaux, P.-O. Cheptou, Flowering plants under global pollinator decline. *Trends in Plant Science* **18**, 353–359 (2013).

51. C. M. Beans, D. A. Roach, An invasive plant alters pollinator-mediated phenotypic selection on a native congener. *American Journal of Botany* **102**, 50–57 (2015).

52. A. P. Hendry, Key questions on the role of phenotypic plasticity in eco-evolutionary dynamics. *Journal of Heredity* **107**, 25–41 (2016).

53. K. M. Winchell, R. G. Reynolds, S. R. Prado-Irwin, A. R. Puente-Rolón, L. J. Revell, Phenotypic shifts in urban areas in the tropical lizard Anolis cristatellus. *Evolution* **70**, 1009–1022 (2016).

54. P. de Villemereuil, O. E. Gaggiotti, M. Mouterde, I. Till-Bottraud, Common garden experiments in the genomic era: new perspectives and opportunities. *Heredity* **116**, 249–254 (2016).

55. D. M. Waller, Environmental Determinants of Outcrossing in Impatiens capensis (Balsaminaceae). *Evolution* **34**, 747–761 (1980).

56. A. H. Hurlbert, S. A. Hosoi, E. J. Temeles, P. W. Ewald, Mobility of Impatiens capensis flowers: effect on pollen deposition and hummingbird foraging. *Oecologia* **105**, 243–246 (1996).

57. J. Schmitt, D. Ehrhardt, D. Swartz, Differential Dispersal of Self-Fertilized and Outcrossed Progeny in Jewelweed (Impatiens capensis). *The American Naturalist* **126**, 570–575 (1985).

58. E. C. Brown de Colstoun, C. Huang, P. Wang, J. C. Tilton, B. Tan, J. Phillips, S. Niemczura, P.-Y. Ling, R. E. Wolfe, Global Man-made Impervious Surface (GMIS) Dataset From Landsat, NASA Socioeconomic Data and Applications Center (SEDAC) (2017); https://doi.org/10.7927/H4P55KKF.

59. J. Régnière, P. Bolstad, Statistical Simulation of Daily Air Temperature Patterns Eastern North America to Forecast Seasonal Events in Insect Pest Management. *Environmental Entomology* **23**, 1368–1380 (1994).

60. K. Al-Shamaa, QBMS: Query the Breeding Management System(s), (2021); https://doi.org/10.32614/CRAN.package.QBMS.

61. J. Burkiewicz, Pollinators of Impatiens capensis in southeastern Canada, version 2.1; https://doi.org/10.5886/wj63qz.

62. H. Wickham, R. François, L. Henry, K. Müller, D. Vaughan, dplyr: A Grammar of Data Manipulation, (2014); https://doi.org/10.32614/CRAN.package.dplyr.

63. P. Mitteroecker, P. Gunz, Advances in Geometric Morphometrics. *Evolutionary Biology* **36**, 235–247 (2009).

64. C. P. Klingenberg, Evolution and development of shape: integrating quantitative approaches. *Nature Reviews Genetics* **11**, 623–635 (2010).

65. M. L. Collyer, D. J. Sekora, D. C. Adams, A method for analysis of phenotypic change for phenotypes described by high-dimensional data. *Heredity* **115**, 357–365 (2015).

66. F. Rohlf, tpsUtil, version 1.83 (2023).

67. F. Rohlf, tpsDig2, version 2.32 (2021).

68. D. C. Adams M. L. Collyer, and A. Kaliontzopoulou, Geomorph: Software for geometric morphometric analyses, (2020); https://cran.r-project.org/package=geomorph.

69. R Core Team, _R: A Language and Environment for Statistical Computing_, version 4.3.3, R Foundation for Statistical Computing (2024); <https://www.R-project.org/>.

70. P. Legendre, L. Legendre, *Numerical Ecology* (Elsevier, 2012).

71. J. Fox, S. Weisberg, B. Price, car: Companion to Applied Regression, (2001); https://doi.org/10.32614/CRAN.package.car.

72. D. Bates, M. Maechler, B. Bolker, S. Walker, lme4: Linear Mixed-Effects Models using "Eigen" and S4, (2003); https://doi.org/10.32614/CRAN.package.lme4.

73. A. F. Zuur, E. N. Ieno, N. J. Walker, A. A. Saveliev, G. M. Smith, *Mixed Effects Models and Extensions in Ecology with R* (Springer, 2009)vol. 574.

74. R. V. Lenth, emmeans: Estimated Marginal Means, aka Least-Squares Means, (2017); https://doi.org/10.32614/CRAN.package.emmeans.

Acknowledgments: In Ottawa, sampling was allowed by the National Capital Comission with permits 23562 in 2021 and 24501 in 2022. In the Silver Creek Conservation Area, sampling was allowed following permits CL22/021. We thank the Koffler Scientific Reserve and staff for access, housing, and help during our sampling. We thank Real Collins and Shirley Dumais for granting access to their propriety in Mirabel. We thank Agiro for granting access to Marais du Nord for sampling, and Domaine de Maizerets for access to sample in Maizerets population. We thank C. Fauteux, M. Vallée, O-L. Kuhn, A. Corkal, and M. Duguay for assisting with fieldwork and data analysis. We thank Guillaume Larocque for his help with the NDVI map. We thank Daniel Schoen for his comments on a previous version of this manuscript.

Funding: This study was supported by the Montreal Botanical Garden, Discovery grants from the Natural Sciences and Engineering Research Council of Canada (NSERC) to S.J. (2018-05027 and 2024-0552), an NSERC Graduate scholarship to J.B., and a MITACS scholarship to S.C. and J.C.

Author contributions:

Conceptualization: SJ, JB

Methodology: JB, SJ, CD

Investigation: JB, JC, SC, JL, EN, SJ

Visualization: JB, SJ, CD, JL

Funding acquisition: SJ

Project administration: JB, SJ

Writing – original draft: JB

Writing – review & editing: JB, JC, SC, JL, EN, CD, SJ

Competing interests: Authors declare that they have no competing interests.

Data and materials availability: All code and data are available on figshare (private upon acceptance) and Canadensys (*61*)

Supplementary Materials

Materials and Methods

Figs. S1 to S7

Tables S1 to S22

References (*55*–*74*)

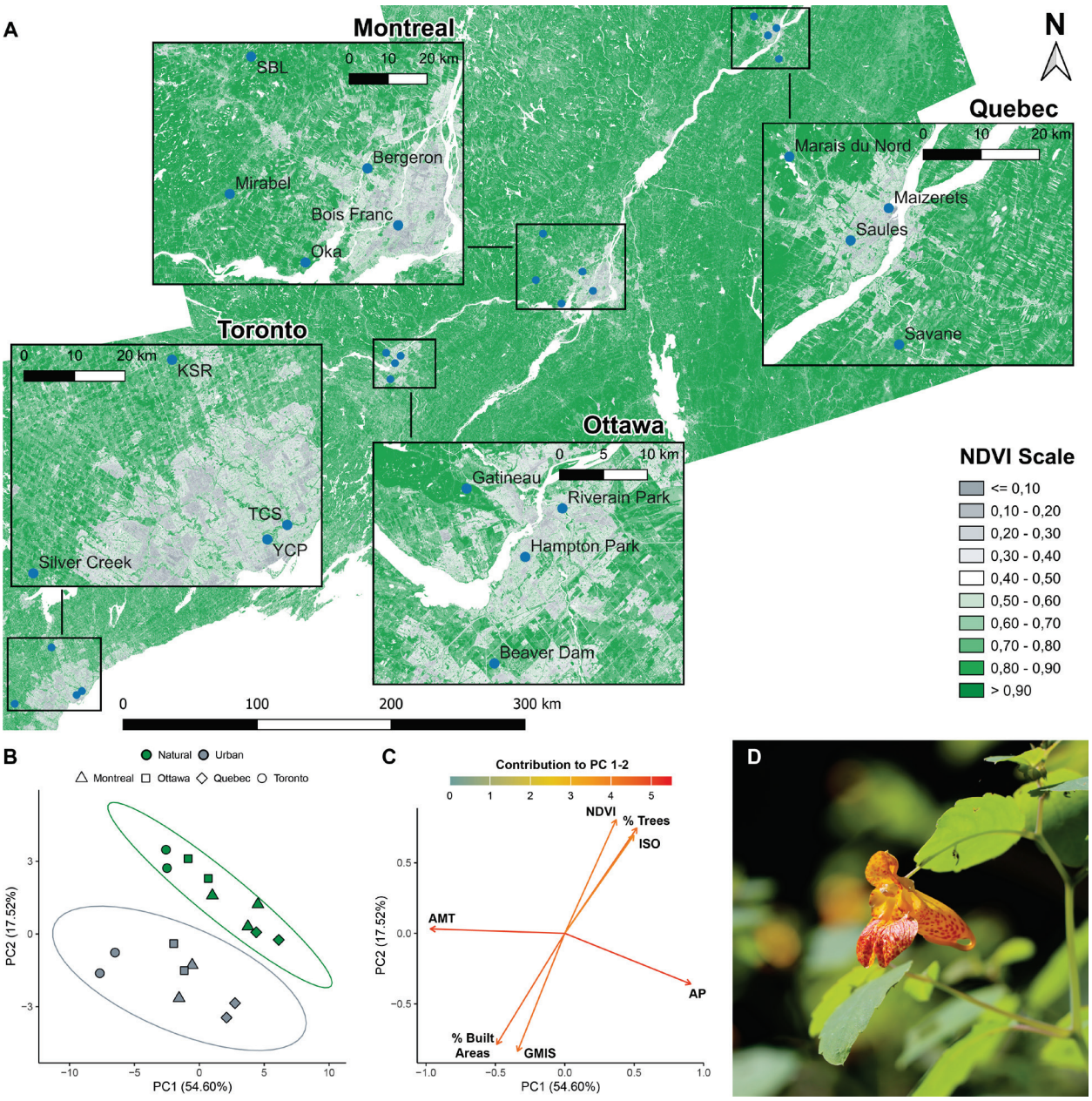

Fig. 1. Study sites and system. Flowers from populations of *Impatiens capensis* were sampled in four regions in 2021 and 2022. (A) Normalized-Difference Vegetation Index (NDVI) map showing the sampled populations; high NDVI values (green) indicate more important vegetation cover. (B) Populations and (C) variables plots of a Principal Component Analysis (PCA) conducted on the mean values of environmental variables from a 500m radius circle around each population. Only the most contributing variables are represented: annual mean temperature (AMT), annual precipitation (AP), isothermality (ISO), NDVI, global man-made impervious surfaces (GMIS), percentage of trees (% Trees) and percentage of built areas (% Built Areas). Ellipses represent 95% confidence interval (CI). PCAs for 1000m and 2000m radius buffers are available in the Supplementary Material. (D) Flower of *Impatiens capensis* (credits: J. Burkiewicz).

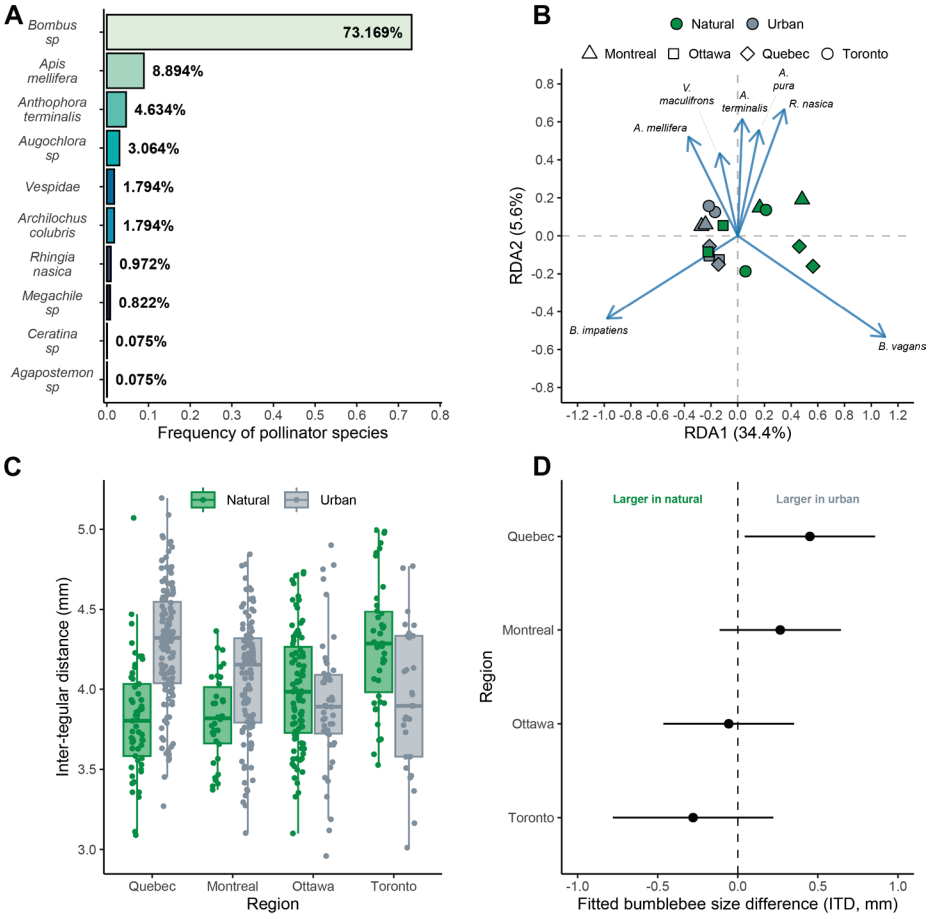

Fig. 2. Characterization of the *I. capensis* pollinator community and size of bumblebees. (A) Relative frequencies of pollinator species computed from video observation data, although frequencies are similar to those obtained with collected specimens (Table S2). (B) Redundancy analysis of pollinator abundance (collected specimens) by habitat and region for the 2022 field season. Only the most abundant species were represented on the graph for clarity purposes. The redundancy analysis on combined field seasons (2021 and 2022) is available in Fig. S2. (C) Boxplots of bumblebee inter-tegular distances by habitat and region, averaged over the two field seasons. Dots represent individual bumblebee measurements; sample sizes are available in Table S4. (D) Estimated marginal means contrasts of bumblebee size between urban and natural habitats for each region from the linear mixed model and associated 95% confidence intervals.

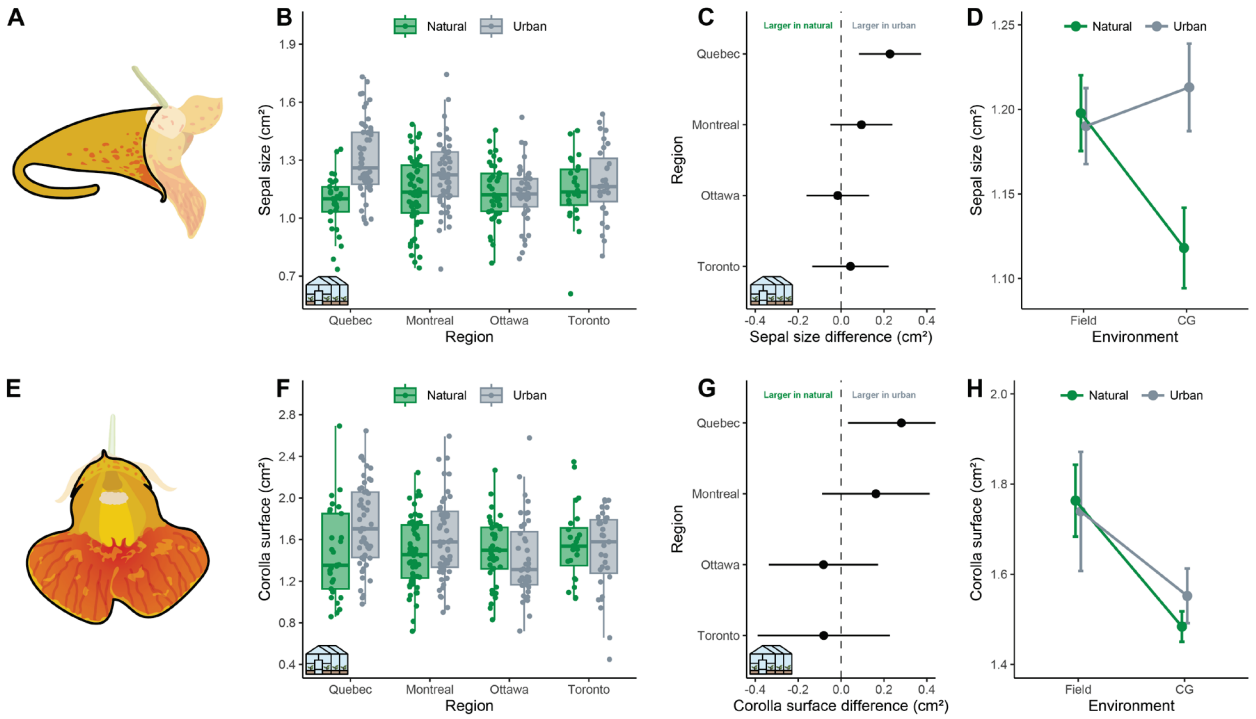

Fig. 3. Sepal size (A-D) and corolla surface (E-H) comparisons between habitats. (A) Drawing showing the measure used to estimate the sepal size of *Impatiens capensis* in black outline. (B) Boxplots of the sepal size measured in the common garden (as indicated by the greenhouse icon) with dots representing individual flowers. (C) Estimated marginal means contrasts of the sepal size between urban and natural habitats per region and associated 95% confidence intervals in the common garden experiment. (D) Mean response of sepal size, grouped by habitats, to environmental change for the 2021 field season. Error bars represent standard errors of the mean. Results with two field seasons combined are available in Fig. S5A. (E) Drawing showing the measure used to estimate the corolla surface of *Impatiens capensis* in black outline. (F) Boxplots of the corolla surface measured in the common garden with dots representing individuals. (G) Estimated marginal means contrasts of the corolla surface between urban and natural habitats per region and associated 95% confidence intervals in the common garden experiment. (H) Mean response of corolla surface, grouped by habitats, to environmental change for the 2021 field season. Error bars represent standard errors of the mean. Results with two field seasons combined are available in Fig. S5B. Credits for the drawings: J. Lafond.

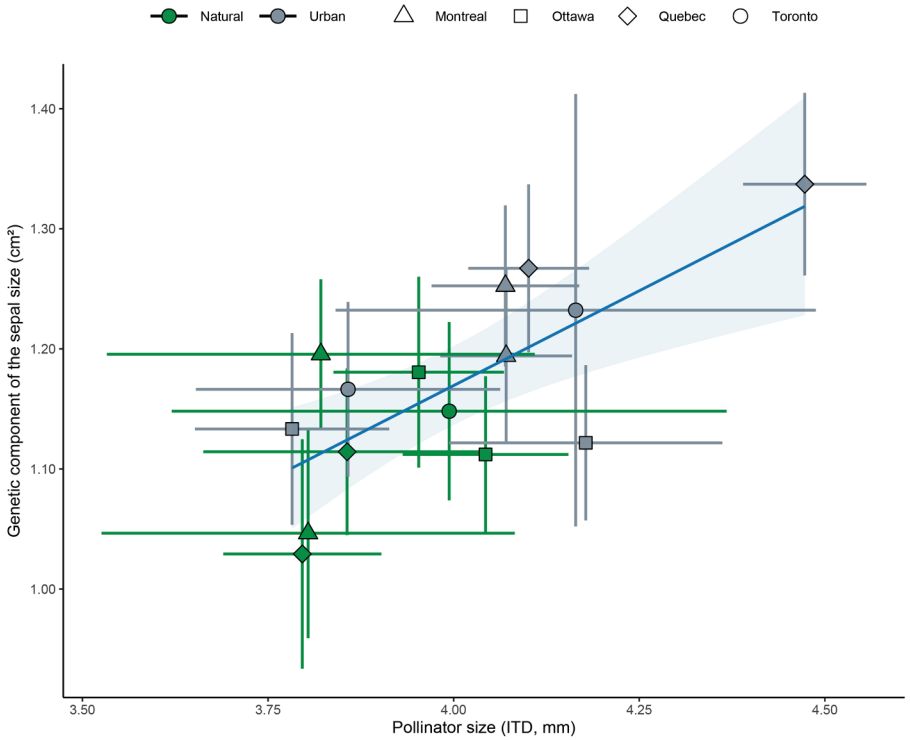

Fig. 4. Correlation between the genetic component of the sepal size and bumblebee inter-tegular distances. The points represent the population mean of the sepal size in the common garden experiment and the population mean bumblebee size averaged across the 2021 and 2022 field seasons. Error bars for the points indicate the 95% confidence intervals of the means. The line shows the significant positive linear relationship with its standard error.

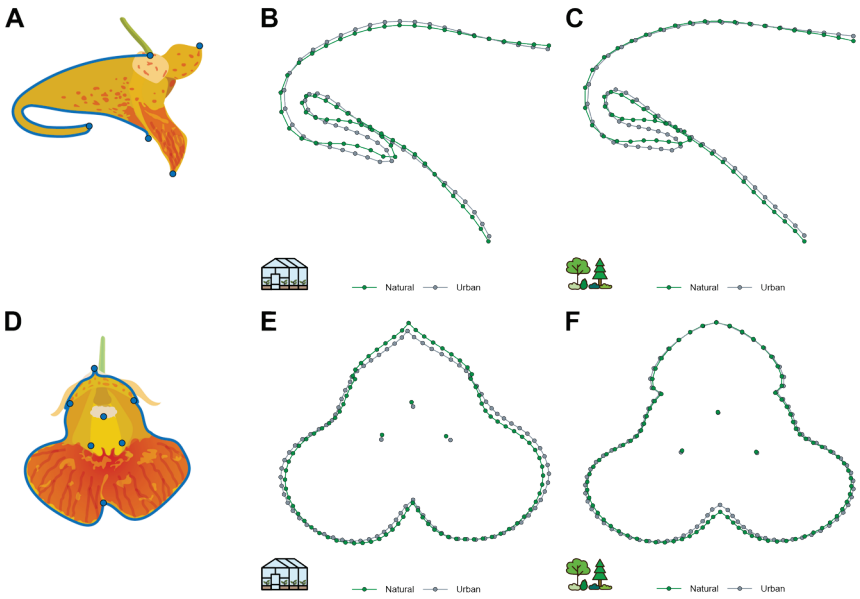

Fig. 5. Predicted posterior sepal and corolla shape comparison between habitats. (A) Drawing showing the landmarks (blue dots) and semilandmarks (blue curves) position on the posterior sepal of *Impatiens capensis*. (B) Predicted shape of the posterior sepal in urban and natural habitats for the common garden experiment. (C) Predicted shape of the posterior sepal in urban and natural habitats for the 2021 field season. (D) Drawing showing the landmarks (blue dots) and semilandmarks (blue curves) position on the corolla of *Impatiens capensis*. (E) Predicted corolla shape in urban and natural habitats for the common garden experiment. (F) Predicted corolla shape in urban and natural habitats for the 2021 field season.

Materials and Methods

Study system

The spotted jewelweed (*Impatiens capensis*) is an herbaceous annual native to eastern North America. It grows in moist to wet environments and ranges from open to closed canopies. When little light falls on plants, they mainly produce cleistogamous flowers, which are closed, tiny, green flowers that self-fertilize (*55*). When ample light falls on plants, they mainly produce chasmogamous flowers, which are large orange protandrous flowers that mainly outcross (*55*). Chasmogamous flowers have three sepals: the two anterior ones are membranous and reduced, and protect the floral bud; the posterior one is saccate and showy, ending with a nectar spur of varying length and curvature. Chasmogamous flowers also have five petals: the two lowers act as a landing pad for insect pollinators, the two laterals guide the pollinators to enter the posterior sepal, and the upper one controls the flower's opening.

Impatiens capensis chasmogamous flowers are pollinated by several functional groups of pollinators, such as bees, ants, wasps, halictid bees, syrphids, and hummingbirds (*37*). Insect pollinators usually land on the lower petals and make contact with the reproductive organs when entering the posterior sepal. Insects can also touch the anthers by feeding on or collecting pollen. The only bird pollinator, *Archilochus colubris,* feeds on nectar and makes contact with the flower reproductive parts with its bill (*56*). Up to 8 seeds can develop in a mature capsule that explodes 1.5 to 4 weeks after fertilization, projecting the seeds up to 2m (*36,39,57*).

Population selection

To test whether urbanization impacted the size and shape of *I. capensis* flowers, we compared urban and natural populations of four large Canadian metropolitan areas (+500,000 inhabitants) within the range of *I. capensis*, which we refer to as “regions”. Using iNaturalist observations and colleagues’ references (*30*), we selected pairs of urban and natural populations of *I. capensis* with more than 100 individuals growing in open canopies in an area of 75 km around the city center of each region. Urban populations had large proportions of impervious surfaces, while natural populations had less impervious surfaces, more vegetation and fewer crop fields around them. We selected 15 populations of *I. capensis* in 2021 and 16 in 2022. One natural population selected in 2021 in the Toronto region eventually produced too few chasmogamous flowers to be kept in the protocol and was abandoned but was replaced with the Silver Creek population in 2022. The Oka

natural population in the Montreal region in 2021 was replaced by the Mirabel population in 2022 because of access issues (Table S1).

Population characterization

The abiotic conditions at each population were characterized with the Normalized Difference Vegetation Index (NDVI), the percentage of land use/land cover, and the mean Global Man-made Impervious Surface (GMIS) (*58*) using satellite images from Sentinel-2 (resolution 10m) or Landsat 7 (resolution 30m). Briefly, we exported the maximum NDVI raster in GeoTIFF for an area covering all selected populations using Google Earth Engine. In QGIS v3.34.6, we merged tiles and removed water from the raster using the lakes, rivers, and coastal waters polygons accessible on the "Open Canada" website (https://open.canada.ca/en). We then projected the maximum NDVI raster to ESPG:3347 – NAD83/Statistics Canada Lambert projected coordinate system. We finally measured the mean NDVI for each population with buffer zones of 500 m, 1000 m, and 2000 m radius centered on them. We followed the same procedure for each population to compute the GMIS and land use percentages for the trees, crops, built areas, bare ground, and range land categories, which represented 100% of land cover for all populations at all spatial scales.

We also characterized each population using bioclimatic variables. We interpolated values of temperature (minimum and maximum, mean, mean minimum and maximum, mean dew), precipitation (total, mean relative humidity, number of wet and dry days), solar radiation, and frost-related metrics (number of days with and without) using BIOSIM 11 (*59*). Briefly, BIOSIM 11 runs a model to assess the variables mentioned above for each population using data from the closest weather station and normal data from the 1980-2010 period to fill the gaps, accounting for latitude, longitude, and elevation. We computed the monthly summary for each population between 2010 and 2022 to obtain average bioclimatic conditions across several years at each site. These values were then imported in R and used to compute worldclim bioclimatic variables using the QBMS package (*60*) for all populations.

We ran a scaled principal component analysis (PCA) including all above abiotic variables. Both urbanization and climatic variables differed, at any spatial scale tested, between natural and urban populations, with urban populations associated with a high proportion of impervious surfaces and built areas, a low proportion of trees, low values of NDVI and high isothermality

(BIO3) and natural populations being opposite (Fig. 1A, C, Fig. S1). Other bioclimatic variables mainly separated the different regions (Fig. 1A, C, Fig. S1).

Field sampling

In both 2021 and 2022, we first visited each population to photograph flowers, collect pollinators, and record flower visitors with cameras, and a second visit allowed us to collect pollinators and record flower visitors again. Both visits were done during peak flowering (between August 1st and September 10th). In each population, we photographed 50 flowers in profile and front view from randomly selected plants with either a Canon T2i with a 60mm macro lens (EF-S 60mm 1:2.8 USM, Canon Inc., Tokyo, Japan) or a Canon 90D with a 100mm macro lens (EF 100mm 1:2.8 L IS USM, Canon Inc., Tokyo, Japan), placing a ruler (unit: centimeter) on the side of the flowers. We also recorded flower visitors for one hour using two GoPro Hero 9 cameras (GoPro, San Mateo, California, USA), placed 2 to 50 m apart to get at least five different flowers at a 30-50 cm distance from the camera to ensure high image quality. Recordings were done in 4K (3820 x 2160) resolution, with 30 frames per second, and linear field of view. In 2021, we also sometimes recorded pollinator visits using a Canon T2i with a 60mm macro lens (EF-S 60mm 1:2.8 USM, Canon Inc., Tokyo, Japan) on a tripod in 1080p (1920 x 1080) resolution at 30 frames per second.

After the cameras stopped recording, two people collected insect pollinators of *I. capensis* for further identification and measurements during 20-minute sessions, using entomological nets while standing in front of, or walking along a stand of *I. capensis*. Pollinators were caught if they touched the reproductive parts of the flower and were then placed in a 50 mL tube in a cooler and frozen at the end of the day. All pollinator observations and captures were conducted in sunny conditions, with a minimum temperature of 15°C and low to no wind.

Common garden experiment

During summer 2021, we collected one seed from at least 30 plants in each population for the common garden experiment. A few days after collection, seeds were stored in Petri dishes on moist filter paper, closed with parafilm, and maintained at 4°C until germination. Seeds were controlled every two weeks for fungal contamination. If needed, we gently cleaned and dried all seeds from the contaminated Petri dish with brown paper and transferred them to a new Petri dish.

Seedlings emerged 4-5 months after being placed in the Petri dishes. Seedlings were transferred to 2-inch square pots containing BM6 multipurpose soil (Berger, Saint-Modeste, Quebec, Canada) and watered every two days from the bottom of the tray, alternating between clear water and fertilized water. We used 15-5-15 NPK fertilizer from Monday to Thursday and 19-2-19 NPK fertilizer from Friday to Sunday. When the plants reached 15 cm in height, they were transferred to 8.5 inch round pots with BM6 soil. They were watered with water and fertilizer every two days, and every day from March 1st. Plants were grown with 16 hours of light, with day and night temperatures of 22°C and 18°C, respectively.

When plants started flowering, we photographed the front and profile views of one random flower on each plant, using a Canon T2i with a 60mm macro lens (EF-S 60mm 1:2.8 USM, Canon Inc., Tokyo, Japan), including a ruler on each picture (Table S1).

Pollinator identification and measurement

Frozen pollinators were pinned on foam blocks using needles of size 00 (0.30 mm diameter), 0 (0.35 mm diameter), or 1 (0.40 mm diameter), depending on pollinator size, and were dried at room temperature for a week. When possible, pollinators were identified at the species level, and genus or family otherwise. Pollinators were then deposited at the Ouellet-Robert entomological collection of the Université de Montréal (*61*).

We used the inter-tegular distance (ITD) as a proxy of pollinator size, as it is a good indicator of insects' dry mass and flight capability (44, 45). We measured it by photographing each pollinator under a Zeiss microscope equipped with an AxioCam HRc (Discovery V20) camera and using the software ZENblue v2.5 Pro (Carl Zeiss, Oberkochen, Germany).

Pollinator observations

When analyzing the videos taken in the field, an animal was marked as a <u>visitor</u> when they either **1)** landed on the flower <u>AND</u> entered the flower, touching the reproductive parts or not, **2)** landed on the petals but did not entered the flower, **3)** landed on the flower and touched the reproductive parts without entering the flower, eating or collecting the pollen, i.e. walking on the reproductive parts, **4)** landed on the flower and ate or collected pollen, and **5)** landed on the flower and stole nectar, or made a hole in the flower. Animals that landed on the posterior sepal and left without

entering the flower, touching the reproductive parts, or trying to steal / rob nectar were not considered visitors.

Among visitors, we further distinguished pollinators from robbers/stealers. Pollinators were visitors that touched the reproductive parts of the flowers, even when eating pollen or just walking on it. Finally, robbers and stealers were visitors that entered the flower without touching the reproductive parts but fed on nectar, or those that made a hole in the spur / posterior sepal, or that exploited such a hole, and fed on nectar without entering the flower by the opening.

When watching recordings, we identified between 5 and 10 open flowers from which we could easily distinguish a pollination or robbing / stealing event. To speed up the process of finding potential pollinators, videos were watched at ×2 speed. When an animal was observed, videos were slowed down (×0.5, ×0.25, or ×0.12 speed) to identify pollinating or robbing/stealing events. For each floral visitor, we recorded the time of the visit, the species or genus and family of the visitor, whether it was a pollinator or a robber/stealer, the number of flowers observed in this particular recording, and the number of flowers visited.

We computed the total observation effort (OE) as the sum over all observation units (eg., one camera recording with a specific number of flowers observed) of the number of hours observed times the number of flowers observed per session:

$$OE = \sum_{observation\ unit} hours\ of\ observation \times number\ of\ flowers\ observed.$$

For instance, if five flowers were observed constantly in a video of two hours (i.e., an observation unit), the observation effort for this observation unit is 10 hours × flower^{-1}. We then calculated the Pollinator Visitation Rate (PVR) as the number of flowers pollinated over the observation effort:

$$PVR = \frac{Number\ of\ flowers\ pollinated}{OE}$$

Using the dplyr package in R (*62*), we computed pollinator visitation rates for each species/genus and population, per species/genus and across populations, and per population for all pollinators. We also calculated the relative frequency of each pollinator taxon as the number of pollination

events observed for that taxon divided by the total number of pollination events, at the population level and over all populations.

Flower shape characterization

We used geometric morphometrics to characterize the flower shape from flower pictures taken in profile and front views, and measure the posterior sepal size and corolla surface (*63–65*). We used tpsUtil v1.83 (*66*) to create .tps files for each population, ensuring specimens for each population were randomly ordered. These .tps files were imported in tpsDig v2.32 (*67*) to digitize specimens. We identified five landmarks (homologous points) for the posterior sepal: 1) the tip of the upper petal, 2) the insertion of the pedicel on the perianth, 3) the extremity of the spur, 4) the lower extremity of the opening of the posterior sepal, and 5) the lower point of the lower petal closer to the camera (Fig. 5A). We also defined two curves with 30 semilandmarks each to capture the shape of the posterior sepal. The first curve followed the outline of the posterior sepal between landmarks 2 and 3 (dorsal curve, Fig. 5A), and the second one followed the outline of the posterior sepal between landmarks 3 and 4 (ventral curve, Fig. 5A).

We placed seven landmarks for the front views of the flowers: 1) the tip of the upper petal, 2) the intersection between the upper petal and the right lateral petal (left for landmark 6, which is symmetrical), 3) the right widest point of the corolla opening (left for landmark 5, which is symmetrical), 4) the intersection of the two lower petals or, if the two petals do not intersect, the center of a segment drawn between the uppermost part of each lower petal, and, 7) the lower point of the stamens or the stigma (Fig. 5D). Note that points 4 and 7 are better defined as semi-homologous landmarks. We also defined four semilandmarks curves to capture the shape of the corolla. The first and fourth followed the outline of the upper petal between landmarks 1 and 2, or 6 and 1, and each contained 10 points. The second and third contained 35 points and followed the lateral and lower petal outline between landmarks 2 and 4, or 4 and 6 (Fig. 5D). Curves were numbered clockwise starting from the top of the flower.

We removed flower pictures that were too blurry or for which critical features of the flowers were masked, preventing us from precisely locating landmarks or semilandmarks. Different persons placed the landmarks, but one person (JB) validated all points and curves of all flowers.

Estimation of flower size

Flower size was estimated from the landmarks and semi-landmarks. For the profile view, the sepal size corresponded to the area of a polygon created by concatenating all curves and landmarks 2, 3, and 4 (Fig. 3A, Fig. 5A). For the front view, the corolla surface corresponded to the area of a polygon created by concatenating all curves and landmarks 1, 2, 4 and 6 (Fig. 3E, Fig. 5D).

Data importation and cleaning

All .tps files were imported in R using the *readland.tps* function from the geomorph package (*68*). For all curves, we removed the first and last semilandmarks because they were redundant with the landmarks. For profile pictures, we also removed landmarks 1 and 5 because they were redundant with the landmarks and semilandmarks of the front pictures and were sometimes challenging to locate precisely. We oriented all images in the same way using the *rotate.coords* function of the geomorph package (*68*).

General Procrustes Analysis (GPA) and technical error

We performed a General Procrustes Analysis (GPA) with the *gpagen* function of the geomorph package (*68*). Briefly, GPA aligns all specimens, minimizing Procrustes distance using rotation, translation, and scaling steps and keeping the difference in shape between individuals (*64*). Semilandmarks were treated as landmarks in the GPA because the high variability of the spur and petals' curvature caused misalignments when treated as semilandmarks (both when minimizing Procrustes distance or using bending energy). We manually checked for outlier shapes to ensure these were not due to improper landmark positioning.

To assess the technical error in landmark positioning, we placed landmarks on duplicate flowers in some populations (four in front view, five in profile view). The technical error estimated using a Procrustes ANOVA with 999 permutations (*procDlm* function of the geomorph package (*68*)) was 0.01% for the profile pictures and 2.08% for the front pictures.

Statistical analyses

We used a combination of linear mixed models, ANOVA, ANCOVA, PERMANOVA (Procrustes ANOVA), and redundancy analysis (RDA) to answer our research questions. We visually inspected normality and homoscedasticity and indicated if these assumptions were unmet and how we treated these cases. All analyses were performed in R version 4.3.3 (*69*).

Pollinator abundance — We evaluated whether pollinator communities differed between urban and natural habitats. Because observation data and collected specimens gave consistent results (Fig. 2A, Table S2), we used only collected specimens for statistical analysis, as insect identifications were more precise because they could be made at the species level. We transformed the community data using Hellinger distances to account for shared absences among sites (*70*). Using a redundancy analysis (RDA), we tested whether we could explain pollinator abundance with regions (cities) and habitats (urban/natural). We performed a full RDA and then performed partial RDA, testing each factor while removing the effect of the other.

Pollinator visitation rate — We assessed whether urbanization influenced pollinator visitation rates. We used region, habitat and their interaction as fixed factors in an ANOVA to explain the variation in pollinator visitation rate, assuming a Gaussian distribution. We tested the significance of region, habitat and their interaction using type II sum of squares (*Anova* function from the car package (*71*)).

Bumblebee size and flower size — We tested whether urbanization affected the sizes (ITD) of bumblebees, the main pollinator, and of flowers (sepal size and corolla surface). We built a complete linear mixed model that included Year (when applicable), Region, Habitat, and their interactions as fixed effects, including a population random effect and allowing slopes to vary with region, habitat, and their interaction.

$$\text{Size} \sim \text{Year} \times \text{Habitat} \times \text{Region} + (\text{Region} \times \text{Habitat} \mid \text{Population})$$

We first selected the best variance structure by fitting and comparing models with random effects of descending order of complexity and all fixed effects. Models were fitted with Restricted Maximum Likelihood (REML) using the *lmer* function from the lme4 R package (*72*) and compared with the *anova* function. Singular models were excluded from the comparison. Models that failed to converge were also excluded from model comparisons. The model with the best variance structure was the one with the lowest AIC (*73*). In all cases, the best variance structure

for the three response variables was a simple population random effect, independent of region or habitat:

$$\text{Size} \sim \text{Year} \times \text{Habitat} \times \text{Region} + (1 \mid \text{Population}).$$

Using this variance structure, we then tested fixed effects and their interactions using type II Wald tests (*Anova* function from the car package (*71*)). We computed estimated marginal means contrasts for urban/natural comparisons within region within year using the Holm correction for multiple testing (*74*).

For flower size, we also tested if the sexual stage of the flowers (male or female) was correlated with the sepal size or the corolla surface, thus eliminating a potential confounding effect. The sexual stage was weakly associated (R^2_{adj} <1%) with sepal size and corolla surface in the field. To test for robustness of the results to the sexual stage, we compared the results of models including or not female flowers (12.2 % of the data) and found consistent results for both analyses (Table S6), meaning our results were not caused by the sexual stage of the flower.

Plasticity of flower size — We tested whether flower size was affected by phenotypic plasticity and if this effect was influenced by urbanization, by comparing the flower size measured in the field to that measured in the common garden. We first analyzed the data from the 2021 field season versus the common garden experiment to compare the phenotype of parents and the phenotype of offspring (the parentage of which is unknown), showing both genetic and plastic responses to environmental change. We then analyzed the data from the 2022 field season versus the common garden experiment to compare the phenotypes of kin, representing the plastic response to environmental change.

For each comparison, we built a linear mixed model to analyze variation in flower size with Environment (either field or common garden), Habitat (either urban or natural), and their interaction as fixed effects, including a population random effect, allowing slopes to vary with environment, habitat, and their interaction. We used the same procedure mentioned in the above ***Bumblebee size and flower size*** section to select the best variance structure. The best model

included a population random effect that changed the intercept and the slopes were allowed to vary with Environment.

$$\text{Size} \sim \text{Environment} \times \text{Habitat} + (\text{Environment} \mid \text{Population})$$

We then tested fixed effects and interactions using type II Wald tests using the *Anova* function from the car package (*71*).

Correlation between bumblebee size and flower size — We tested whether variation in mean population sepal sizes could be explained by variation in mean population bumblebee sizes (ITD), i.e. if we could find a general mechanism to explain variation among populations. We used the sepal sizes measured in the common garden because they correspond to the genetic component of this trait and analyzed their variation with an analysis of covariance with habitat and ITD and their interaction as fixed factors:

$$\text{Sepal Size} \sim \text{Habitat} \times \text{ITD}.$$

We tested the significance of the habitat, ITD and interaction using the *Anova* function from the car package (*71*), with type II sum of squares, and computed R^2_{adj} using the *lm* function. We also removed potential confounding effects between the explanatory variables by fitting the same model on centered values of ITD per habitat. We found consistent results, meaning that the ITD effect was not driven by differences in ITD between habitats.

Correlation between pollinator visitation rates and flower size — We tested whether variation in mean population corolla surfaces correlates with variation in mean population pollinator visitation rates, using the averaged rates over the two field seasons (to get a more precise estimate). We used the corolla surfaces measured in the common garden because they correspond to the genetic component of this trait and analyzed their variation by building an ANCOVA with habitat and pollinator visitation rates and their interaction as fixed factors:

$$\text{Corolla Surface} \sim \text{Habitat} \times \text{Pollinator Visitation Rate}.$$

We tested the significance of the habitat, pollinator visitation rates and interaction using the *Anova* function from the car package (*71*), with type II sum of squares, and computed R^2_{adj} using the *lm* function.

Flower shape—We used a Procrustes ANOVA (equivalent to a PERMANOVA) with the *procD.lm* function from the geomorph package (*68*) to test whether flower shape was influenced by size (allometry effect), year (when applicable), sexual stage of the flower (male vs female), region, and habitat, including all possible interactions between these variables:

$$\text{Shape} \sim \text{Size} \times \text{Year} \times \text{Sex} \times \text{Region} \times \text{Habitat}.$$

Because Procrustes ANOVA cannot include random factors, we followed Collyer et al. 2015 (*65*) recommendations and used the interaction of habitat and population as the error term to test for fixed effects on interpopulation variation. We removed all non-significant interactions except the one between habitat and region, which we were interested in. We reran a Procrustes ANOVA on a simpler model with the remaining terms. We used type 1 Procrustes ANOVA, ordering factors in a way that we tested for the effect of habitat and the interaction between habitat and region after all other factors.

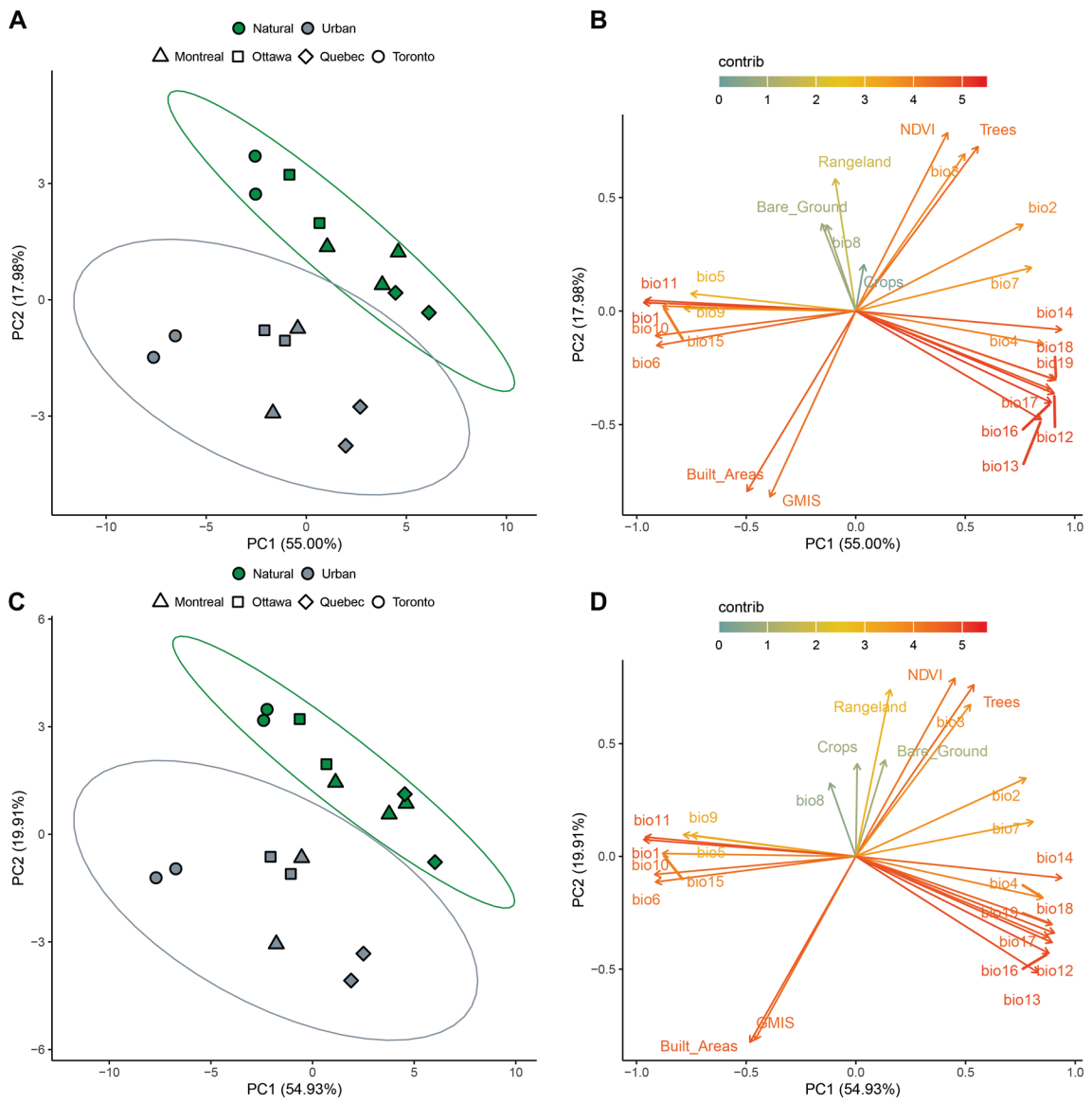

Fig. S1. Population characteristics at different spatial scales. (A-B) Individual and variables plot of a Principal Component Analysis (PCA) on urbanization and bioclimatic variables computed using a circle of 1000m radius around each population. (C-D) Individual and variables plot of a Principal Component Analysis (PCA) on urbanization and bioclimatic variables computed using a circle of 2000m radius around each population. Urban and natural populations mainly differ in the percentage of impervious surfaces, trees and isothermality (BIO3) in both analyses, whereas cities vary according to temperatures and precipitations.

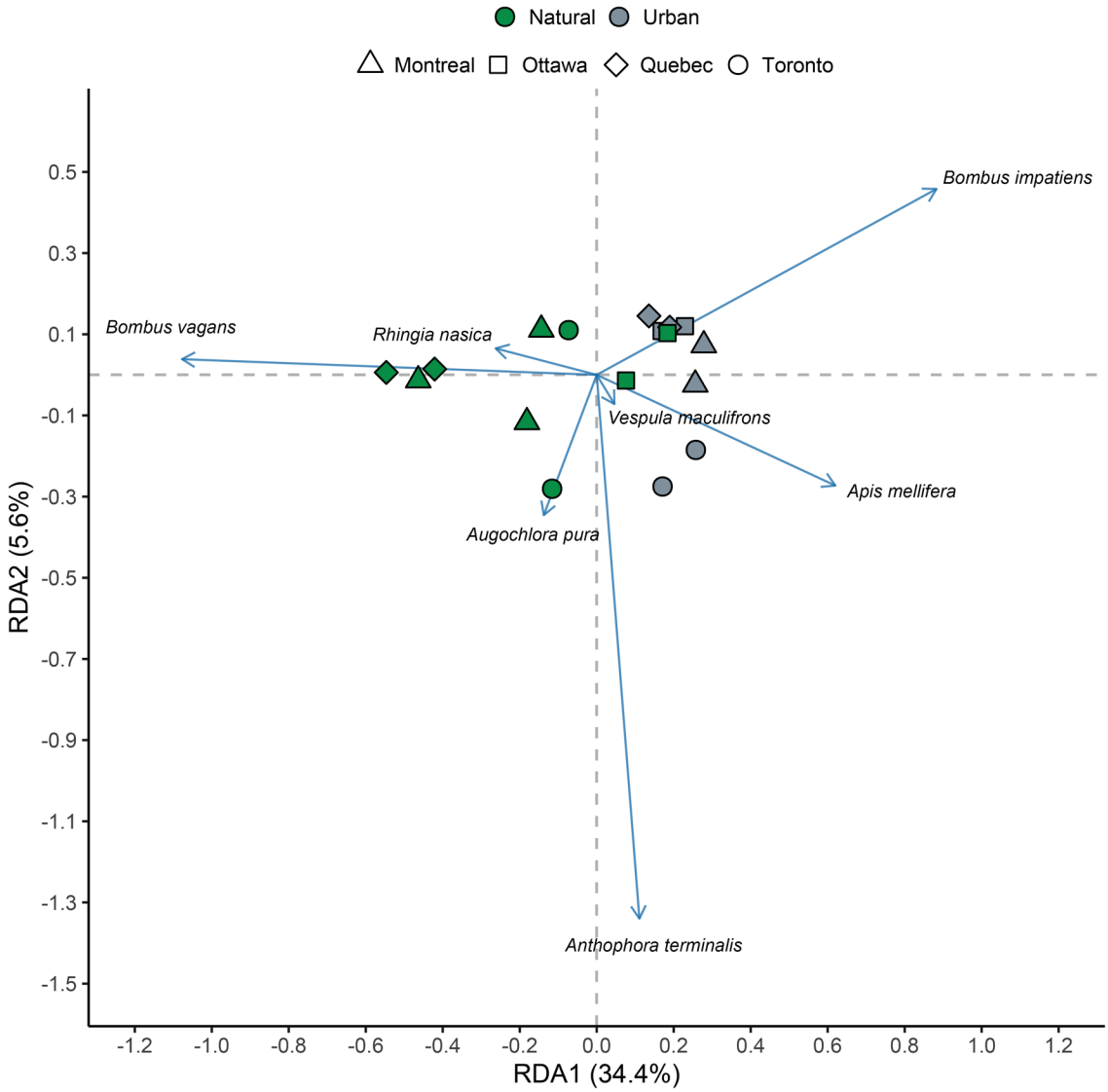

Fig. S2. Redundancy analysis (RDA) evaluating the impact of urbanization on the *Impatiens capensis* pollinator community in 2021 and 2022. When both years are considered together, the main difference between urban and natural habitats is the bumblebee species pollinating *I. capensis*. *Anthophora terminalis* separates the Toronto region because it was overrepresented in this region in 2021.

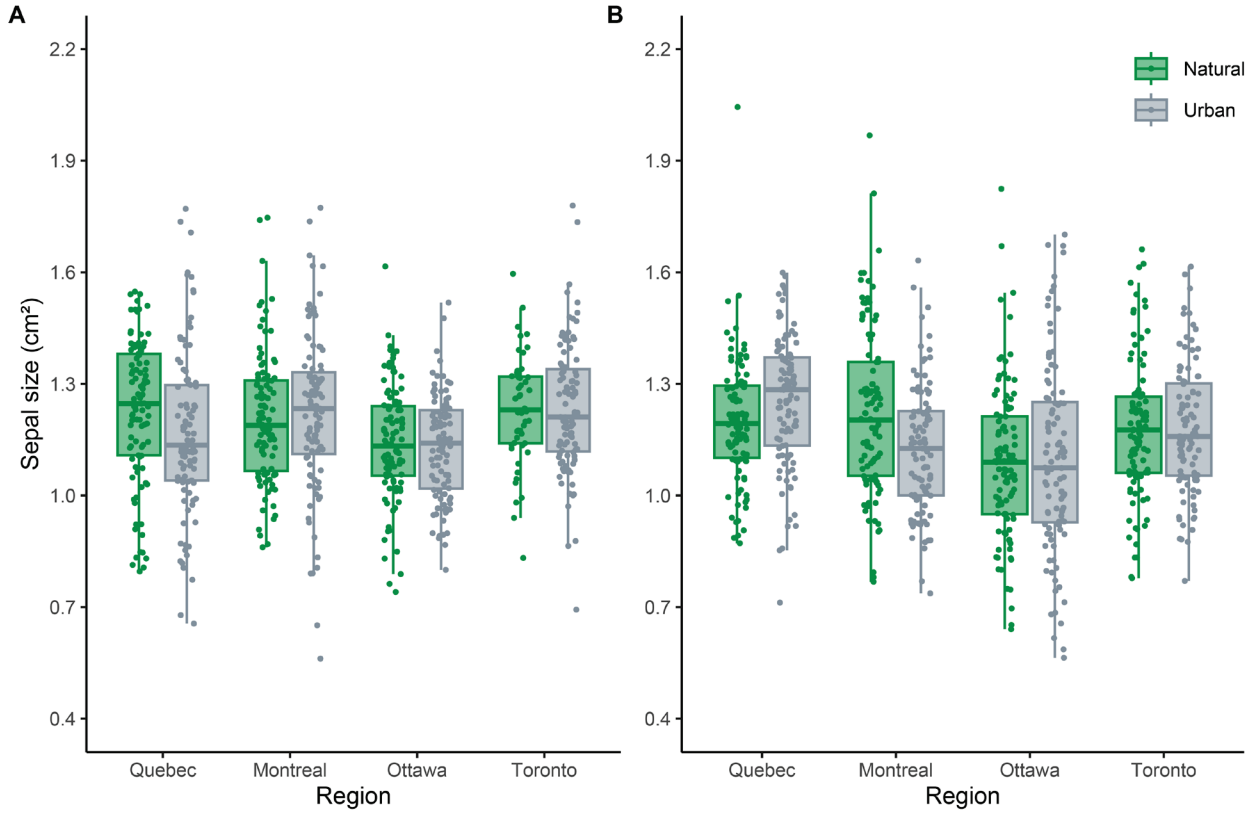

Fig. S3. Sepal size in the field according to region and habitat type for 2021 (A) and 2022 (B). See Table S1 for more information about sampling.

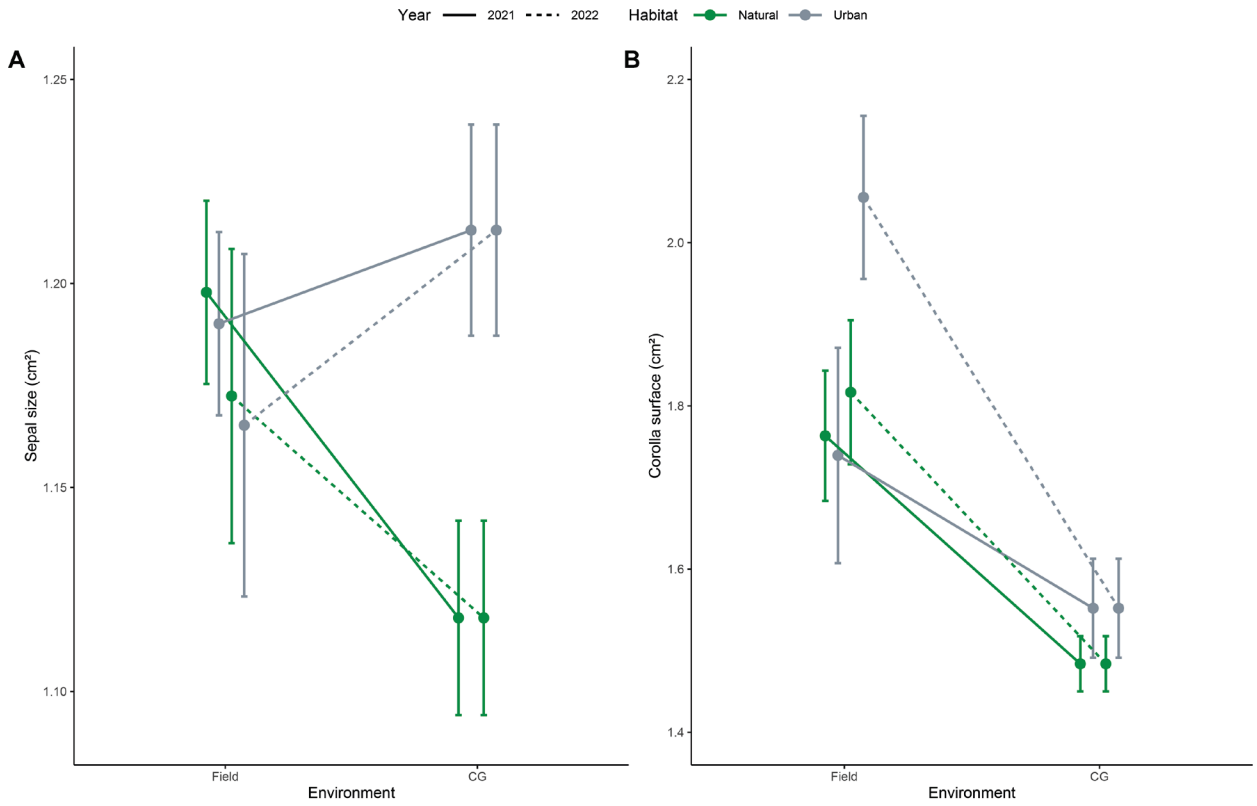

Fig. S4. Mean response of sepal size (A) and corolla surface (B) to environment change, grouped by habitat. Solid lines represent 2021 data in the field compared to the unique common garden experiment, and dashed lines represent 2022 data in the field compared to the unique common garden experiment.

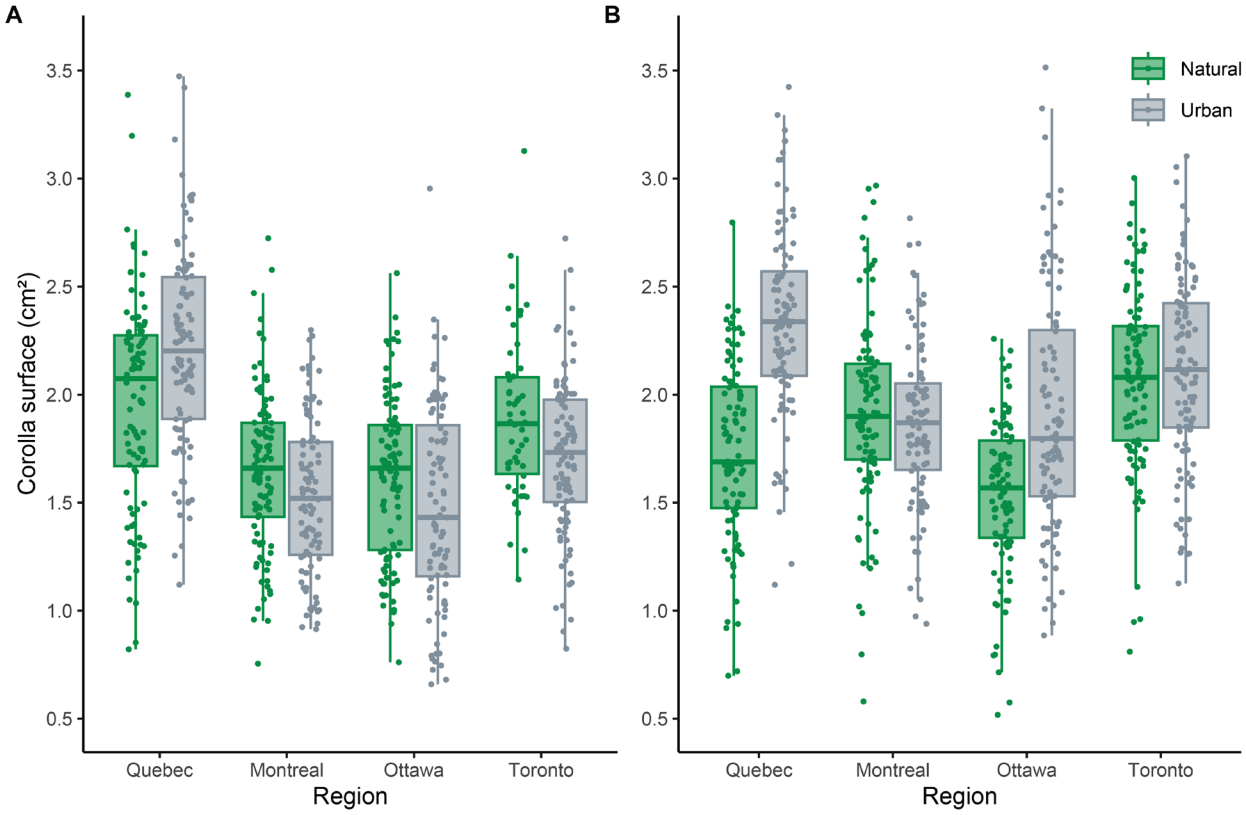

Fig. S5. Corolla surface in the field according to region and habitat type for 2021 (A) and 2022 (B). See Table S1 for more information about sampling.

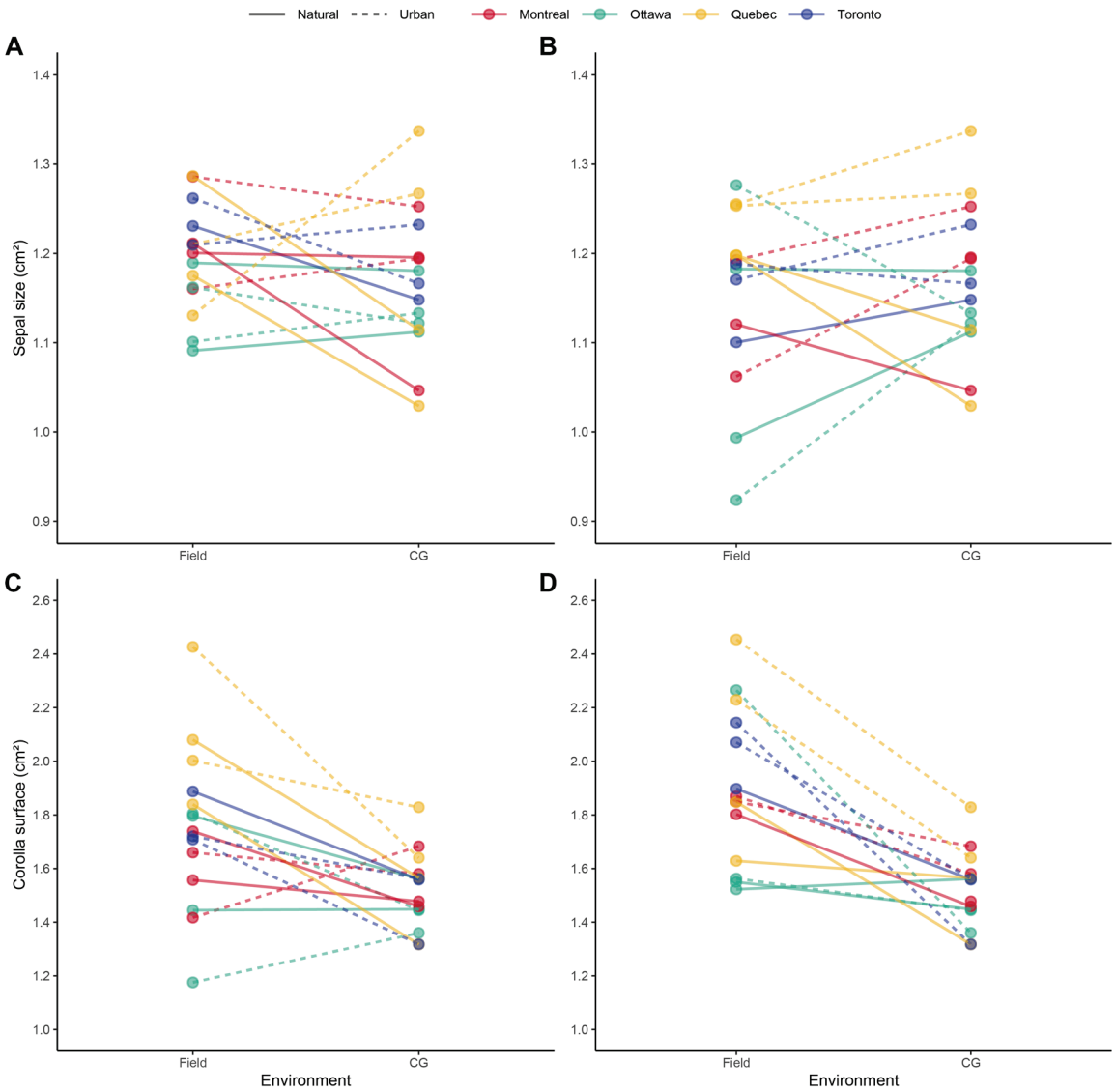

Fig. S6. Plastic response of sepal size and corolla surface, grouped by region. Lines represent populations colored according to their region. Solid lines represent natural populations, and dashed lines represent urban populations. (A) Sepal size response for 2021 field data vs common garden data. (B) Sepal size response for 2022 field data vs common garden data. (C) Corolla surface response for 2021 field data vs common garden data. (D) Corolla surface response for 2022 field data vs common garden data.

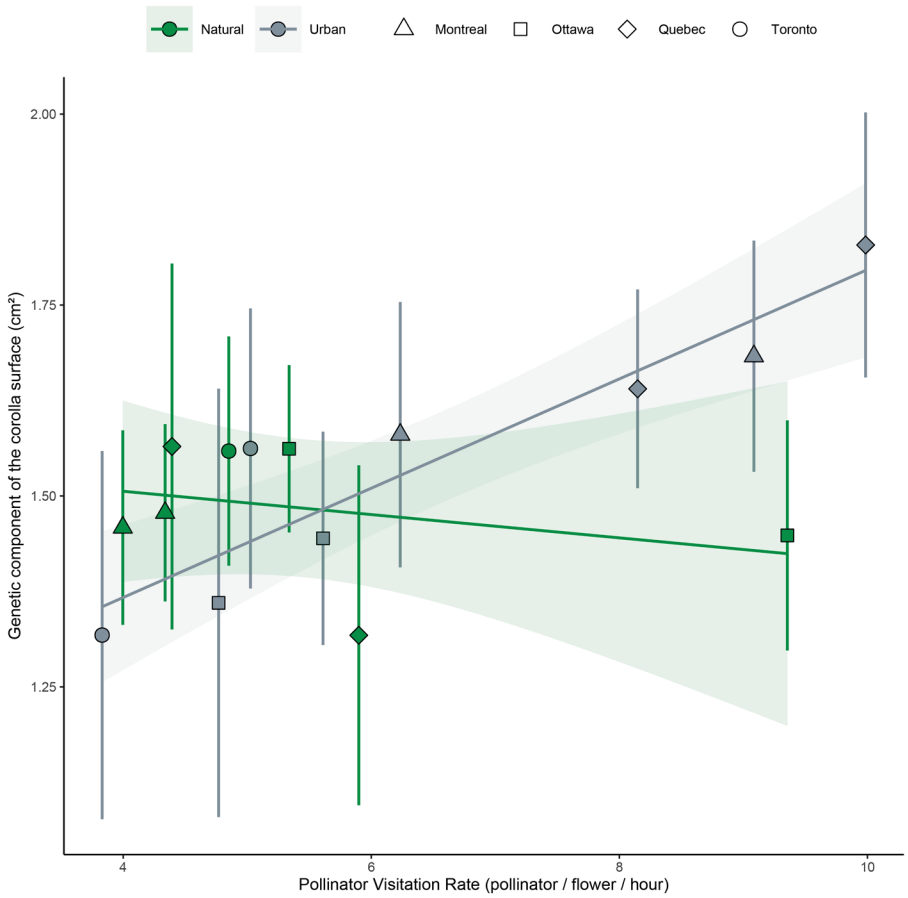

Fig S7. Correlation between the genetic component of the corolla surface and the pollinator visitation rate. There was a significant effect of the pollinator visitation rate on corolla surface, and a significant interaction between pollinator visitation rate and habitat. Regression lines for urban and natural populations are shown, with their standard errors. The points represent the population mean of the corolla surface in the common garden experiment (with 95% confidence intervals of the mean) and the population mean of the pollinator visitation rate averaged across the 2021 and 2022 field seasons.

Table S1. Populations studied. The first number in the sample size column is for the 2021 field season, the second one for the 2022 field season, and the third for the common garden experiment. The first line in the sample size column for each population is for profile pictures (sepal), and the second one is for front pictures (corolla).

Population	Region	Habitat	Latitude	Longitude	Sample size
Bergeron (BER)	Montreal	Urban	45.651	-73.753	50/50/26 44/50/27
Bois Franc (BFC)	Montreal	Urban	45.505	-73.708	49/49/28 49/49/28
Mirabel (MIR)	Montreal	Natural	45.683	-74.213	NA/50/NA NA/50/NA
Oka (OKA)	Montreal	Natural	45.482	-74.035	49/NA/39 48/NA/39
SBL (SBL)	Montreal	Natural	45.974	-74.020	50/50/21 49/49/21
Beaver Dam (DAM)	Ottawa	Natural	45.293	-75.823	50/49/25 50/50/25
Gatineau (GAT)	Ottawa	Natural	45.474	-75.798	50/50/14 50/50/14
Hampton Park (HAM)	Ottawa	Urban	45.391	-75.740	50/50/27 47/50/27
Riverain Park (RIV)	Ottawa	Urban	45.429	-75.670	50/50/13 49/50/13
Maizerets (MAI)	Quebec	Urban	46.838	-71.211	50/50/30 50/50/28
Marais du Nord (MDN)	Quebec	Natural	46.963	-71.388	47/50/17 48/50/17
Saules (SAU)	Quebec	Urban	46.81	-71.316	47/50/25 50/50/25
Savane (SAV)	Quebec	Natural	46.633	-71.287	50/49/12 48/49/12
KSR (KSR)	Toronto	Natural	44.029	-79.528	50/50/24 50/50/24
Silver Creek (SCK)	Toronto	Natural	43.703	-79.964	NA/50/NA NA/50/NA
TCS (TCS)	Toronto	Urban	43.701	-79.328	49/50/9 50/50/9
YCP (YCP)	Toronto	Urban	43.682	-79.383	50/50/22 50/50/22

Table S2. Pollinator relative frequency calculated on collected specimens. The 2022 collection effort was more important (see Material and Methods), and this explains why more specimens were observed. NA are for species not found in either 2021 or 2022. Values are rounded.

Species	Frequency		
	2021 (n = 171 insects)	**2022** (n = 521 insects)	**Cumulated** (n=692 insects)
Agapostemon virescens	NA	0.002	0.001
Ancistrocerus adiabatus	NA	0.002	0.001
Anthophora terminalis	0.070	0.036	0.045
Apis mellifera	0.088	0.056	0.064
Augochlora pura	0.018	0.015	0.016
Bombus borealis	0.012	NA	0.003
Bombus fervidus	0.006	0.002	0.003
Bombus impatiens	0.596	0.633	0.624
Bombus ternarius	0.018	0.002	0.006
Bombus vagans	0.099	0.136	0.127
Calliphoridae	NA	0.004	0.003
Ceratina calcarata	NA	0.002	0.001
Dolichovespula arenaria	0.023	0.012	0.014
Ectemnius continuus	NA	0.004	0.003
Epistrophe sp.	NA	0.002	0.001
Megachile mendica	0.006	0.002	0.003
Megachile relativa	NA	0.002	0.001
Muscidae	NA	0.002	0.001
Platycheirus nearcticus	NA	0.013	0.010
Rhingia nasica	NA	0.019	0.014
Toxomerus geminatus	NA	0.004	0.003
Unknown Syrphidae	NA	0.002	0.001
Unknown Vespula	0.006	NA	0.001
Vespula acadica	0.006	NA	0.001
Vespula alascensis	NA	0.002	0.001
Vespula consobrina	0.041	0.004	0.013
Vespula flavipilosa	NA	0.002	0.001
Vespula germanica	NA	0.004	0.003
Vespula maculifrons	0.012	0.036	0.030

Table S3. Analysis of the pollinator visitation rate variation

A) Analysis of variance table for Pollinator Visitation Rate

	Pollinator Visitation Rate			
Effect	Sum of Squares	df	F	P
Region	18.75	3	1.433	0.258
Habitat	3.77	1	0.865	0.362
Region × Habitat	48.09	3	3.675	**0.026**

B) Estimated marginal means contrasts (Urban - Natural)

Urban - Natural contrast	**estimate**	**t**	**df**	**P**
Quebec	3.92	2.654	23	0.056
Montreal	2.07	1.399	23	0.430
Ottawa	-2.24	-1.515	23	0.430
Toronto	-1.23	-0.769	23	0.449

Table S4. Sample size and summary of bumblebee sizes. This table summarizes the 2021 and 2022 sampling years combined. n is the sample size for each population, and N is the sample size for each habitat within a region.

Population	Habitat	Region	n	ITD	sd	se	ci	N
MDN	Natural	Quebec	19	3.857	0.402	0.092	0.194	57
SAV	Natural	Quebec	38	3.796	0.324	0.053	0.106	
MAI	Urban	Quebec	63	4.473	0.33	0.042	0.083	128
SAU	Urban	Quebec	65	4.101	0.328	0.041	0.081	
MIR	Natural	Montreal	19	3.828	0.239	0.055	0.115	34
OKA	Natural	Montreal	7	3.821	0.311	0.118	0.288	
SBL	Natural	Montreal	8	3.804	0.333	0.118	0.278	
BER	Urban	Montreal	30	4.071	0.238	0.043	0.089	102
BFC	Urban	Montreal	72	4.07	0.423	0.05	0.099	
DAM	Natural	Ottawa	45	4.043	0.371	0.055	0.112	87
GAT	Natural	Ottawa	42	3.953	0.368	0.057	0.115	
HAM	Urban	Ottawa	16	4.178	0.345	0.086	0.184	49
RIV	Urban	Ottawa	33	3.782	0.369	0.064	0.131	
KSR	Natural	Toronto	6	3.994	0.356	0.145	0.374	42
SCK	Natural	Toronto	36	4.331	0.382	0.064	0.129	
TCS	Urban	Toronto	8	4.164	0.387	0.137	0.323	29
YCP	Urban	Toronto	21	3.858	0.45	0.098	0.205	

Table S5. Analysis of the bumblebee size variation.

A) Wald χ^2 test			
	Inter-Tegular Distance (ITD, mm)		
Effect	**χ^2**	**df**	**P**
Year	0.109	1	0.74
Region	2.075	3	0.556
Habitat	2.414	1	0.12
Year × Region	1.989	3	0.574
Year × Habitat	0.302	1	0.582
Region × Habitat	8.826	3	**0.031**
Year × Region × Habitat	1.494	3	0.683

B) Estimated marginal means contrasts (Urban - Natural)				
	Inter-Tegular Distance (ITD, mm)			
Urban - Natural contrast	**estimate**	**t**	**df**	**P**
Quebec	0.45	2.599	7.21	0.138
Montreal	0.264	1.584	9	0.443
Ottawa	-0.056	-0.324	7.45	0.754
Toronto	-0.279	-1.141	28.29	0.526

We tested whether bumblebee inter-tegular distance (ITD) was explained by Year (2021 or 2022), Region (Quebec, Montreal, Ottawa, or Toronto), Habitat (Urban or Natural), and all interactions between these factors, using linear mixed models. **A)** Result of the Wald chi-square test **B)** We estimated the effect of habitat on inter-tegular distance for each region using post-hoc tests comparing estimated marginal means contrasts. We corrected for multiple comparisons using the holm correction.

Table S6. Analyses of the sepal size and corolla surface variation in the field.

A) Wald χ2 test, male only						
	Sepal Size			Corolla Surface		
Effect	χ^2	**df**	**P**	χ^2	**df**	**P**
Year	8.385	1	**0.003**	33.597	1	**<0.001**
Region	3.834	3	0.279	37.237	3	**<0.001**
Habitat	0.344	1	0.557	2.191	1	0.138
Year × Region	28.021	3	**<0.001**	25.117	3	**<0.001**
Year × Habitat	8.146	1	**0.004**	54.977	1	**<0.001**
Region × Habitat	0.302	3	0.959	16.120	3	**0.001**
Year × Region × Habitat	6.980	3	0.072	10.690	3	**0.013**

B) Estimated marginal means contrasts (Urban - Natural), male only								
	Sepal Size				Corolla surface			
Urban - Natural contrast	**estimate**	**t**	**df**	**P**	**estimate**	**t**	**df**	**P**
Quebec 2021	-0.060	-0.646	9.36	1.000	0.293	2.363	10.3	0.234
Quebec 2022	0.067	0.719	9.43	1.000	0.623	4.992	10.6	**0.004**
Montreal 2021	-0.059	-0.678	10.08	1.000	-0.167	-1.386	12.2	0.572
Montreal 2022	-0.068	-0.781	10.15	1.000	-0.007	-0.056	12.4	1.000
Ottawa 2021	-0.027	-0.291	9.45	1.000	-0.223	-1.776	10.8	0.416
Ottawa 2022	-0.008	-0.080	9.48	1.000	0.364	2.905	10.7	0.103
Toronto 2021	-0.081	-0.826	11.39	1.000	-0.271	-1.905	16.2	0.374
Toronto 2022	0.012	0.130	9.66	1.000	0.018	0.140	11.4	1.000

C) Wald χ2 test, male and female						
	Sepal Size			Corolla Surface		
Effect	χ^2	**df**	**P**	χ^2	**df**	**P**
Year	17.529	1	**<0.001**	45.646	1	**<0.001**
Region	3.720	3	0.293	33.065	3	**<0.001**
Habitat	0.239	1	0.624	2.279	1	0.131
Year × Region	24.444	3	**<0.001**	25.008	3	**<0.001**
Year × Habitat	6.151	1	**0.013**	63.618	1	**<0.001**
Region × Habitat	0.302	3	0.959	14.239	3	**0.002**
Year × Region × Habitat	6.806	3	0.078	6.638	3	0.084

D) Estimated marginal means contrasts (Urban - Natural), male and female								
	Sepal Size				Corolla surface			
Urban - Natural contrast	**estimate**	**t**	**df**	**P**	**estimate**	**t**	**df**	**P**
Quebec 2021	-0.060	-0.672	9.48	1.000	0.255	2.005	10.4	0.358
Quebec 2022	0.057	0.630	9.44	1.000	0.604	4.756	10.4	**0.006**
Montreal 2021	-0.044	-0.527	10.14	1.000	-0.183	-1.501	12.1	0.636
Montreal 2022	-0.066	-0.784	10.14	1.000	0.003	0.021	11.9	1.000
Ottawa 2021	-0.009	-0.097	9.43	1.000	-0.137	-1.078	10.4	0.916
Ottawa 2022	0.012	0.131	9.44	1.000	0.378	2.975	10.3	0.094
Toronto 2021	-0.068	-0.728	10.92	1.000	-0.311	-2.234	14	0.254
Toronto 2022	-0.001	-0.009	9.43	1.000	0.034	0.266	10.3	1.000

We tested whether sepal size or corolla surface was explained by Year (2021 or 2022), Region (Quebec, Montreal, Ottawa, or Toronto), Habitat (Urban or Natural), and all interactions between these factors using linear mixed models. Because the Sex factor was associated with sepal size and corolla surface in the field, we decided to run the same models with males only **(A-B)** and male and female **(C-D)** to assess the effect of females on our results**.** For each test (either male only or male and female combined), we estimated the effect of habitat on the sepal size and corolla surface for each region using post-hoc tests comparing estimated marginal means contrasts. We corrected for multiple comparisons using holm correction.

Table S7. Analyses of the sepal size and corolla surface variation in the common garden experiment.

A) Wald χ^2 test

	Sepal size			Corolla surface		
Effect	**χ^2**	**df**	**P**	**χ^2**	**df**	**P**
Region	2.270	3	0.084	5.113	3	0.163
Habitat	8.564	1	**0.003**	2.683	1	0.101
Region × Habitat	8.329	3	**0.039**	8.136	3	**0.043**

B) Estimated marginal means contrasts (Urban - Natural)

	Sepal Size				Corolla surface			
Urban - Natural contrast	**estimate**	**t**	**df**	**P**	**estimate**	**t**	**df**	**P**
Quebec	0.227	3.700	7.29	**0.028**	0.281	2.617	7.78	0.126
Montreal	0.095	1.660	5.42	0.459	0.162	1.709	4.61	0.459
Ottawa	-0.015	-0.249	7.13	1	-0.082	-0.762	7.02	0.942
Toronto	0.043	0.585	6.91	1	-0.081	-0.623	6.84	0.942

We tested whether the sepal size or corolla surface was explained by Region (Quebec, Montreal, Ottawa, or Toronto), Habitat (Urban or Natural), and the interaction between these factors, using linear mixed models. **A)** Result of the Wald chi-square test **B)** We estimated the effect of habitat on the sepal size and corolla surface for each region using post-hoc tests comparing estimated marginal means contrasts. We corrected for multiple comparisons using holm correction.

Table S8. Analysis of the mean responses of sepal size and corolla surface, grouped by habitats, to environment change.

	Sepal Size						Corolla size					
	2021			2022			2021			2022		
Effect	χ^2	**df**	**P**	χ^2	**df**	**P**	χ^2	**df**	**P**	χ^2	**df**	**P**
Environment	0.916	1	0.338	0.047	1	0.837	8.859	1	**0.002**	36.761	1	**<0.001**
Habitat	2.003	1	0.156	4.052	1	**0.044**	1.445	1	0.229	2.492	1	0.114
Environment × Habitat	4.796	1	**0.028**	3.706	1	0.054	0.519	1	0.471	1.486	1	0.222

We tested whether the sepal size or corolla surface was explained by Environment (Field or Common Garden), Habitat (Urban or Natural), and the interaction between these factors, using linear mixed models. The comparison between the common garden and the 2021 field season represents the effect of genetic and plastic changes on the two components of flower size (in the common garden, we measure the offspring of seeds collected in the field in 2021). In 2022, we compared the same generation to one another (assessing the plasticity more than the genetic changes). Therefore, we ran separate models for 2021 and 2022.

Table S9. Analysis of the relationship between the genetic component of sepal size variation and bumblebee inter-tegular distances

	Sepal size			
Effect	Sum of Squares	df	F	P
Habitat	0.006	1	1.742	0.213
ITD	0.022	1	6.531	**0.026**
Habitat × ITD	0.000005	1	0.001	0.971

Table S10. Analysis of the relationship between the genetic component of corolla surface variation and the visitation rate of pollinators

	Corolla surface			
Effect	Sum of Squares	df	F	P
Habitat	0.001	1	0.288	0.601
Pollinator Visitation Rate	0.085	1	13.2	**0.003**
Habitat × Pollinator Visitation Rate	0.096	1	14.851	**0.002**

Table S11. Analysis of the flower shape variation in the common garden experiment and in the field.

A) Procrustes ANOVA on flower shape, excluding the "environment" factor.

		Factors	Df	MS	Rsq	F	P
Sepal	**Common garden**	Size	1	0.48813	0.03662	5.7409	**0.002**
		Sex	1	0.09369	0.00703	1.1019	0.350
		Region	3	0.10132	0.02280	1.1916	0.350
		Habitat	1	0.07298	0.00547	0.8583	0.502
		Region×Habitat	3	0.08595	0.01934	1.0108	0.454
		Habitat×Population	7	0.08503	0.04465	1.0000	1.000
	Field	Size	1	3.01023	0.04240	6.6537	**0.007**
		Year	1	0.17214	0.00242	0.3805	0.854
		Sex	1	0.27642	0.00389	0.6110	0.695
		Region	3	1.74981	0.07394	3.8677	**0.005**
		Habitat	1	1.69706	0.02390	3.7511	**0.019**
		Region×Habitat	3	0.56702	0.02396	1.2533	0.337
		Habitat×Population	9	0.45242	0.05735	1.0000	1.000
Corolla	**Common garden**	Size	1	1.37494	0.10318	13.5472	**0.001**
		Sex	1	0.49330	0.03702	4.8604	**0.007**
		Region	3	0.03944	0.00888	0.3886	0.980
		Habitat	1	0.04430	0.00332	0.4365	0.837
		Region×Habitat	3	0.04251	0.00957	0.4189	0.972
		Habitat×Population	7	0.10149	0.05331	1.0000	1.000
	Field	Size	1	2.07279	0.04042	8.8874	**0.002**
		Year	1	0.42192	0.00823	1.8090	0.154
		Sex	1	0.52744	0.01029	2.2615	0.104
		Region	3	0.55914	0.03271	2.3974	**0.036**
		Habitat	1	0.20683	0.00403	0.8868	0.472
		Region×Habitat	3	0.38019	0.02224	1.6301	0.156
		Habitat×Population	10	0.23323	0.04548	1.0000	1.000

B) Procrusts ANOVA on corolla surface only, including the "environment" factor

Factors	Df	MS	Rsq	F	P
Size	1	4.0716	0.0605	17.4631	**0.001**
Year	1	0.8022	0.01192	3.4406	0.043
Sex	1	0.6576	0.00977	2.8204	0.059
Region	3	0.5287	0.02357	2.2674	0.061
Habitat	1	0.3917	0.00582	1.6800	0.162
Environment	1	1.4451	0.02147	6.1981	**0.002**
Region×Habitat	3	0.2377	0.0106	1.0194	0.424
Habitat×Population	9	0.2332	0.03118	1	1

A) We used Procrustes ANOVA (PERMANOVA) to assess the effect of habitat on flower shape. We constructed a model with Size, Year, Sex, Region, Habitat, and the interactions between these factors as explanatory variables of sepal or corolla shape. We omitted the Year term for the common garden as we ran the experiment once. We compute results using type I Procrustes ANOVA, meaning that the effect of Habitat is assessed after all other factors. We also added population nested in habitat in the model; this way, we were able to define the error of the ANOVA as the mean square of population nested in habitats instead of residuals, therefore considering populations as the statistical individual. This conservative approach offers us more confidence in detecting differences between habitats. **B)** We assessed the effect of the environment factor (Field vs Common Garden) on corolla shape using the same rationale as in **A)**

Tables S12-S22 are provided in supplementary file Table_S12_S22.xlsx

Table S12. The effect of habitat, region, year and all interactions on bumblebee inter-tegular distance. We show the estimate, standard error and t value for each factor level and interaction, compared to the intercept.

Table S13. The effect of habitat, region and all interactions on sepal size in the common garden experiment. We show the estimate, standard error and t value for each factor level and interaction, compared to the intercept.

Table S14. The effect of habitat, region, year and their interaction on sepal size in the field, for male only flowers. We show the estimate, standard error and t value for each factor level and interaction, compared to the intercept.

Table S15. The effect of habitat, region, year and interactions on sepal size in the field, for male and female flowers. We show the estimate, standard error and t value for each factor level and interaction, compared to the intercept.

Table S16. The effect of environment, urbanization and their interaction on sepal size in 2021. We show the estimate, standard error and t value for each factor level and interaction, compared to the intercept.

Table S17. The effect of environment, urbanization and their interaction on sepal size in 2022. We show the estimate, standard error and t value for each factor level and interaction, compared to the intercept.

Table S18. The effect of habitat, region and all interactions on corolla surface in the common garden experiment. We show the estimate, standard error and t value for each factor level and interaction, compared to the intercept.

Table S19. The effect of habitat, region, year and their interaction on corolla surface in the field, for male only flowers. We show the estimate, standard error and t value for each factor level and interaction, compared to the intercept.

Table S20. The effect of habitat, region, year and interactions on corolla surface in the field, for male and female flowers. We show the estimate, standard error and t value for each factor level and interaction, compared to the intercept.

Table S21. The effect of environment, urbanization and their interaction on corolla surface in 2021. We show the estimate, standard error and t value for each factor level and interaction, compared to the intercept.

Table S22. The effect of environment, urbanization and their interaction on corolla surface in 2022. We show the estimate, standard error and t value for each factor level and interaction, compared to the intercept.